Review Article

Lopamudra Giri, Smruti Rekha Rout, Rajender S. Varma, Michal Otyepka*, Kolleboyina Jayaramulu*, and Rambabu Dandela*

Recent advancements in metal–organic frameworks integrating quantum dots (QDs@MOF) and their potential applications

https://doi.org/10.1515/ntrev-2022-0118
received December 17, 2021; accepted April 5, 2022

Abstract: Design and development of new materials and their hybrids are key to addressing current energy issues. Thanks to their tunable textural and physiochemical properties, metal–organic frameworks (MOFs) show great potential toward gas sorption, catalysis, sensing, and electrochemical energy applications. Nevertheless, practical applications of MOFs have been hampered because of their limited electrical conductivity, micropore size, and poor stability. However, smart integration of zero-dimensional quantum dots (QDs) into an MOF template, where the host structure offers suitable interactions for enhancing the stability and synergic properties, may be a solution. The objective of this review is to summarize recent advances in the field of QD@MOFs, highlighting fresh approaches to synthesis strategies and progress made in their application to optoelectronic devices, sensing, biomedical, catalysis, and energy storage. The current challenges and future directions of QDs@MOFs hybrids toward advancing energy and environmental applications are also addressed. We anticipate that this review will inspire researchers to develop novel MOF hybrids for energy, optoelectronics, and biomedical applications.

Keywords: metal–organic frameworks, quantum dots, hybrids, catalysis, sensing, water purification, optoelectronic device, supercapacitors

1 Introduction

Metal–organic frameworks (MOFs) have garnered tremendous attention from the research community, following the pioneering effort of Yaghi *et al.* that opened the floodgates to extending this field of research [1–8]. So far, the resounding success of these high surface area materials with tunable active sites has triggered infinite motivation for seeking newly fashioned materials with more unique properties that would meet current challenges [9–18]. Comprehensive research into MOFs regarding their distinctive behavior and their physical characteristics is frequently published [19–25]. The development and fabrication of MOFs into application-specific forms, such as nanostructures [26–34], reinforced membranes [35–44], and capsules [45–53] have become a subject of interest for researchers. MOF-based hybrid composites are also widely studied through mixing MOFs with several other materials, such as ceramics, natural polymers, nanomaterials, and proteins, which result in the evolution of novel well-designed products with improved functionalities [54–60].

Formally, zero-dimensional (0D) semiconductor nanocrystal materials comprising groups II–VI, III–V, or IV elements with a diameter of 2–10 nm are denoted as quantum dots (QDs) and have acquired considerable interest due to their excellent size-dependent tunable electronic properties

* **Corresponding author: Michal Otyepka,** Regional Centre of Advanced Technologies and Materials, Czech Advanced Technology and Research Institute (CATRIN), Palacký University Olomouc, Šlechtitelů 27, 783 71 Olomouc, Czech Republic; IT4Innovations, VSB – Technical University of Ostrava, 17. Listopadu 2172/15, 708 00 Ostrava-Poruba, Czech Republic, e-mail: michal.otyepka@upol.cz
* **Corresponding author: Kolleboyina Jayaramulu,** Regional Centre of Advanced Technologies and Materials, Czech Advanced Technology and Research Institute (CATRIN), Palacký University Olomouc, Šlechtitelů 27, 783 71 Olomouc, Czech Republic; Department of Chemistry, Indian Institute of Technology Jammu, Jammu & Kashmir, 181221, India, e-mail: jayaramulu.kolleboyina@iitjammu.ac.in
* **Corresponding author: Rambabu Dandela,** Department of Industrial and Engineering Chemistry, Institute of Chemical Technology-Indian Oil Bhubaneswar Campus, Bhubaneswar, India, e-mail: r.dandela@iocb.ictmumbai.edu.in
Lopamudra Giri, Smruti Rekha Rout: Department of Industrial and Engineering Chemistry, Institute of Chemical Technology-Indian Oil Bhubaneswar Campus, Bhubaneswar, India
Rajender S. Varma: Regional Centre of Advanced Technologies and Materials, Czech Advanced Technology and Research Institute (CATRIN), Palacký University Olomouc, Šlechtitelů 27, 783 71 Olomouc, Czech Republic

and budding applications in the areas of sensing, catalysis, nano-medicine, and bio-imaging [61–67]. In most cases, this 0D material consists of core (*e.g.*, InP, TiO_2, GaAs, CdS)–shell (*e.g.*, CdS ZnS, PbS, ZnO) structures encompassing a combination of a large number of atoms comprising mainly groups 12–16 (like ZnSe, ZnO, CdSe, *etc.*) or 13–15 (InP, InAs, *etc.*) [68–73]. Despite its several benefits, this form of QDs has a cytotoxic effect on live cells and tissues. To solve the shortcomings of traditional QDs, a new generation of QDs was designed, such as Si QDs, Ag_2Se QDs, carbon dots (CDs), graphene QDs (GQDs), and perovskite. Recently, perovskite QDs have gained popularity in the field of electric and optoelectronics due to their adjustable bandgap, high light-absorption efficiency, high photoluminescence (PL) quantum yield, *etc.* [74–77]. Furthermore, these 0D materials can be simply modified by the surface modification method. Importantly, most of QDs are sustainable in aqueous systems and have coatings that comprise various functional groups, such as alcohols, amines, thiols, and carboxylic acids. Interestingly, a wide range of covalently conjugated molecules has been developed utilizing these functional groups. Moreover, because of the enormous surface area and quantum detention upshot, these materials have some advantages juxtaposed with traditional chromophores, such as extensive absorption bands, low photobleaching, thin and even emission bands, extended lifetimes, and high quantum yields [78–82]. Although QDs have excellent properties, the easy agglomeration of QDs leads directly to fluorescence quenching, which restricts their utilization in various fields [83–86]. Considerable effort has been invested in overcoming this hurdle, for example, passivation with an additional semiconductor film with a suitable bandgap, embedment of QDs with a variety of material (*e.g.*, polymers or micelles), casing QDs with silica shell to harvest QDs@SiO_2 composites, *etc.* [87–95]. However, all these methods are time-consuming and could lead to the formation of unwanted products or undesired behavior in the system. To provide QDs with multifunctional functionality, attempts to encapsulate these semiconductor nanoparticles and adjustable composite architectures must be investigated. Surprisingly, MOFs with high porosity and specific surface area provide an exciting platform, creating an ideal environment for loading QDs and preventing them from aggregation. At the same time, QDs enhance the physicochemical properties of MOFs. As a result, the amalgamation of QDs and MOFs results in good dispersion and great stability. In this context, MOF-derived QDs (QDs@MOF) have piqued curiosity and opened up a new avenue for a variety of applications [75,77,96–100]. These hybrid materials have captivating properties, such as outstanding PL, excellent biocompatibility, good mechanical/thermal stability, and relative simplicity of functionalization [101–106]. As displayed in Figure 1a, the number of papers on QDs@MOF has increased dramatically in recent years, particularly since 2016. A large variety of QDs@MOF materials have evolved, and their characteristics and intriguing applications have been studied ever since (Figure 1b). Although the research on QDs@MOFs is increasing (Table 1), there have been only a few review articles in this research field so far. In view of this flourishing research area, we have summarized the QDs@MOF fabrication strategy, its unique properties, and the wide-ranging applications, and we believe that this review will unfold the path toward newer innovative research and diverse applications.

2 Fabrication strategy for QDs@MOF

Various fabrication strategies have been adopted for the synthesis of QDs@MOF over the last decade. Normally, the strategies comprise two customized methods, "ship-in-a-bottle" (ship–bottle) and "bottle-around-the-ship" (bottle–ship), and the additional two approaches are "photo deposition" and "direct surface functionalization" (Figure 2), which are deliberated in the following section.

2.1 Ship–bottle

The ship–bottle approach (Figure 2) involves the immobilization of small molecules or QDs precursors in the pore windows of MOFs followed by further treatment to attain the desired structure. Various methodologies, such as vapor deposition, solution infiltration, and solid-state grinding, have been employed to introduce QD precursors into MOFs, although precisely controlling the location, content, structure, and morphology of the incorporated guests is sometimes quite challenging. Based on the synthesis condition, the ship–bottle technique is further categorized into three types including "solution infiltration," "chemical vapor infiltration," and "double solution method." In this context, Gao *et al.* [107] employed the abovementioned strategies and developed CdS QDs encapsulated in NH_2-MIL-125 through two steps, including the addition of NH_2-MIL-125 to TiO_2 solution to acquire NH_2-MIL-125@TiO_2 and further inclusion of CdS QDs solution to as-synthesized solubilized NH_2-MIL-125@TiO_2 to form

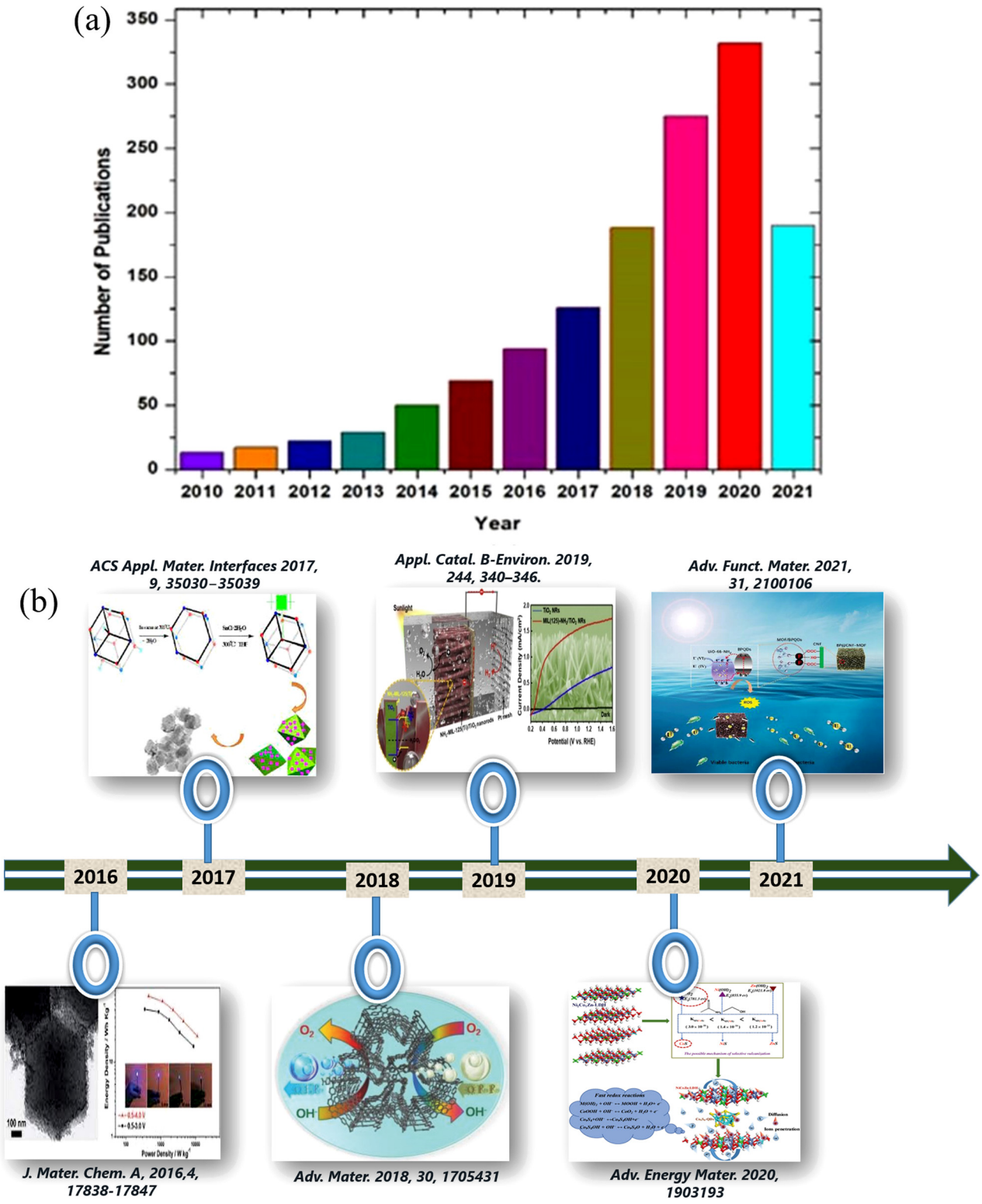

Figure 1: (a) The number of journal articles published on QDs@MOF (source: ISI Web of Knowledge, 2010s to 2021); (b) the outline depicts recent advances in the creation of several QDs@MOFs.

CdS/NH_2-MIL-125@TiO_2 (Figure 3a). Similarly, Gao *et al.* [108] prepared a SnO_2@ZIF-8 composite by the immersion of ZIF-8 into the SnO_2 QD precursors followed by the addition of hydrogen peroxide. Furthermore, Zhang *et al.* [109]

Table 1: List of documented QDs@MOF, including the type of QDs and MOF, utilized their preparative methods and their potential applications in various fields

Sr. no.	MOF	QDs	Method	Application		Ref.
1	Eu-MOFs	CDs	Bottle–ship	Cr(VI) detection	Sensing	[124]
2	MIL-125(Ti)	Ag_2S/CdS/CuS QDs	Photochemical deposition	Cr(VI) reduction		[114]
3	MIL-53(Fe)	CDs	Ship–bottle	Cr(VI) reduction		[133]
4	ZIF-8	CDs/AuNCs	Ship–bottle	Hg(II) detection		[134]
5	Eu-MOFs	CDs	Bottle–ship	Hg(II) detection		[135]
6	Eu-MOFs	N-doped CDs	Bottle–ship	Ag^+ detection		[136]
7	ZIF-8	CDs	Bottle–ship	Cu^{2+} detection		[137]
8	UiO-66-NH_2	CDs	Bottle–ship	Cu^{2+} detection		[138]
9	ZIF-67	Polyethylene glycol (PEG)-capped ZnS QDs	Bottle–ship	Cu^{2+} detection		[139]
10	ZIF-8	CDs	Ship–bottle	Fe^{3+} detection		[140]
11	ZIF-8	Nitrogen-doped graphene QDs (N-GQDs)	Ship–bottle	Fe^{3+} detection		[141]
12	Zn-MOFs	CDs	Ship–bottle	Cu^{2+} and Fe^{3+} detection		[142]
13	UIO-66-NH_2	CDs	Ship–bottle	Cu^{2+} and quinalphos detection		[138]
14	MOF-5	$CH_3NH_3PbBr_3$ QDs	Ship–bottle	Heavy metal ion detection		[143]
15	In-MOFs	CDs	Bottle–ship	Moisture and water detection in organics		[144]
16	ZIF-365	CdTe QDs	Ship–bottle	L-Histidine and Cu^{2+} detection		[125]
17	ZIF-8	CDs	Bottle–ship	Dopamine detection		[126]
18	ZIF-8	Mn:ZnS	Sol–gel	Chlorpyrifos detection		[145]
19	UiO-66	Amine-functionalized carbon QDs	Ship–bottle	4-Nitrophenol detection		[128]
20	HKUST-1	CDs	Bottle–ship	Catechol detection		[127]
21	IRMOF-3	Nitrogen-doped CDs	Ship–bottle	Trinitrotoluene detection		[146]
22	MOF-76	CDs	Ship–bottle	2,6-Pyridinedicarboxylic acid detection		[147]
23	MIL-101(Cr)	GQDs	Ship–bottle	Benzene and toluene detection		[148]
24	Cu-MOFs	Carbon nitride QDs	Ship–bottle	Isoniazid detection		[149]
25	IRMOF-3	N-GQDs	Bottle–ship	Procalcitonin detection		[150]
26	ZIF-8	B-CDs/P-CDs	Ship–bottle	Triticonazole detection		[151]
27	MOF-5	CdS QDs	Bottle–ship	Cardiac troponin I detection		[152]
28	Fe(III)-MIL-88B-NH_2	ZnSe QDs	Bottle–ship	Antigen detection		[112]
29	MIL-100(Fe)	BNQDs	Ship–bottle	Antibiotics removal		[153]
30	MIL-101(Fe)	CDs	Ship–bottle	6-Mercaptopurine detection		[154]
31	ZIF-8	CdTe QDs	Bottle–ship	Oxidase activities detection		[155]
32	UiO-66-NH_2	BPQDs	Template-assisted method	Uranium extraction		[106]
33	Zn-MOFs	Graphitic carbon nitrides QDs	Ship–bottle	Riboflavin detection		[156]
34	Zr-MOF	CdTe QDs	Ship–bottle	Ascorbic acid detection		[157]
35	ZIF-8	CDs	Ship–bottle	Ascorbic acid and ascorbate oxidase detection		[158]
36	Zr-MOFs	GQDs	Bottle–ship	Aflatoxins detection		[159]
37	MIL-101(Cr)	CdSe QDs	Ship–bottle	Alpha-fetoprotein detection		[160]
38	ZIF-8	CDs	Ship–bottle	Quercetin detection		[161]
39	Fe-BDC	N, S-GQDs	Drop casting	Histamine detection		[162]
40	Tb-MOF (MOF-76)	Boric acid-modified CDs	Ship–bottle	2,6-Pyridinedicarboxylic acid detection		[147]
41	MIL-53	CDs	Ship–bottle	Diaminotoluene detection		[163]
42	MIL-101-SO_3H	Amino-CQDs	Ship–bottle	2,4-Dinitrophenol detection		[164]
43	ZIF-8	CdTe QDs	Bottle–ship	NO detection		[165]
44	UiO-66-$(COOH)_2$	CDs	Ship–bottle	Temperature sensing		[166]

(*Continued*)

Table 1: *Continued*

Sr. no.	MOF	QDs	Method	Application		Ref.
45	Eu-MOFs	N,S-CDs	Bottle–ship	Detection of water in organic solvents		[167]
46	UiO-66-NH_2	CDs	Ship–bottle	Water treatment membranes		[168]
47	ZIF-8	GQDs	Ship–bottle	Removal of malachite green		[55]
48	Ru-MOFs	CdS QDs	Drop casting	Electrochemiluminescence sensor		[120]
49	MIL-100(Fe)	CdS QDs	*In situ* consecutive chemical bath deposition	Degradation of bisphenol		[169]
50	MIL-53	Carboxymethylcellulose/ graphene QDs matrix	Bottle–ship	Anticancer drug carrier	Bio-medical	[170]
51	MIL-68(In)	Zn-Ag-In-S QDs	Bottle–ship	Screening of anticancer drug activity		[171]
52	MIL-101-NH_2	BPQDs	Ship–bottle	Photothermal therapy		[131]
53	ZIF-8	GQDs	Bottle–ship	Chemo- and photothermal therapy		[132]
54	ZIF-8	CDs	Bottle–ship	Drug delivery		[129]
55	ZIF-8	DOX-MIPs	Bottle–ship	Drug delivery		[130]
56	IRMOF-3	CDs	Bottle–ship	Drug delivery		[172]
57	UiO-66-NH_2	CDs	Ship–bottle	Bio-imaging		[173]
58	ZIF-8	CdS QDs	Bottle–ship	Bio-imaging		[174]
59	ZIF-8	CDs	Ship–bottle	Drug delivery		[175]
60	UiO-66-NH_2	CDs	Bottle–ship	Drug delivery		[176]
61	ZIF-8	CDs	Bottle–ship	Photodynamic therapy		[177]
62	ZIF-8	CDs	Bottle–ship	Monitoring of cell apoptosis		[178]
63	$[Zn(HCOO)_3][C_2H_8N]$,	Nitrogen-doped CDs (N-CQDs)	Physical fusion	Antimicrobial activity		[179]
64	Cu-ZIF-8	CDs	Bottle–ship	Peroxidase mimics for assaying GSH		[99]
65	PCN-224(Ni)	CdS QDs	Ship–bottle	Hydrogen evolution	Catalysis	[180]
66	UiO-66 (UiOS-Cu)	CdS/ZnS QDs	Ship–bottle	Hydrogen evolution		[181]
67	PCN-222 and PCN-221	Pt/C QDs	Ship–bottle	Hydrogen evolution		[182]
68	UiO-66-$(SH)_2$	CdS QDs	Ship–bottle	Hydrogen evolution		[183]
69	MIL-101	CdS, CDs	Ship–bottle	Hydrogen evolution		[110]
70	NU-1000	CdS QDs	Photo deposition	Hydrogen evolution		[86]
71	UIO-66-NH_2	MoS_2 QDs	Direct deposition	Hydrogen evolution		[184]
72	La-MOFs	CdSe QDs	Direct surface functionalization	Hydrogen evolution		[185]
73	MIL-100(Fe)	GQDs	Ship–bottle	CO_2 reduction		[186]
74	Zn-Bim-His	GQDs	Ship–bottle	CO_2 reduction		[187]
75	MIL-125(Ti)	g-C_3N_4/CuO	Ship–bottle	CO_2 reduction		[188]
76	ZIF-8/ZIF-67	$CsPbBr_3$ QDs	Bottle–ship	CO_2 reduction		[189]
77	UIO-66(NH_2)	$CsPbBr_3$ QDs	Ship–bottle	CO_2 reduction		[74]
78	PCN-221(Fe)	$MAPbI_3$ QDs	Ship–bottle	CO_2 reduction		[190]
79	Ni-MOFs	Ti_3C_2 QDs	Bottle–ship	Nitrogen reduction		[191]
80	Zn/Co bimetallic ZIF	Co QDs	Pyrolysis	Oxygen reduction reaction		[192]
81	CoNi-bimetallic MOF	Ag QDs	Ship–bottle	Oxygen reduction reaction		[97]
82	Ni-MOFs	CDs	Bottle–ship	Oxygen evolution reaction		[193]
83	Fe-MOFs	Pt (1 1 1)	Bottle–ship	Electrocatalyst for water splitting		[59]

(*Continued*)

Table 1: *Continued*

Sr. no.	MOF	QDs	Method	Application		Ref.
84	UiO-66-NH_2	GQDs	Spray coating	Photocatalyst		[194]
85	UiO-66-NH_2	GQDs	Ship–bottle	Photocatalyst		[105]
86	ZIF-8	CDs	Simple dispersion	Photocatalyst		[195]
87	ZIF-8	CdS QDs	Ship–bottle	Photocatalyst		[196]
88	MIL-125-NH_2	CdS QDs	Ship–bottle	Photocatalyst		[107]
89	In-MIL-68	BiO QDs	Ship–bottle	Photocatalyst		[197]
90	PCN-333(Fe)	$CsPbBr_3$ QDs	Ship–bottle	Photocatalyst		[75]
91	NH_2-UiO-66	$Cs_3Bi_2I_9$ QDs	Ship–bottle	Photocatalyst		[77]
92	UiO-66	S,N GQDs	Ship–bottle	Photocatalyst		[198]
93	NH_2-MIL-125(Ti)	CDs	Ship–bottle	Photocatalyst		[199]
94	MIL-101(Cr)	SnO_2	Ship–bottle	Photocatalyst		[200]
95	ZIF-8@MIL-68(In)	ZnO QDs	Calcination	Photocatalyst		[201]
96	Eu-MOFs	CdTe QDs	Direct surface functionalization	Dye disintegration (Rh 6G)		[202]
97	NTU-9	CdTe QDs	Bottle–ship	Dye disintegration (Rh 6G)		[203]
98	UIO-66	CdSe QDs	Ship–bottle	Dye disintegration (RhB)		[204]
99	MIL-125	CdSe QDs	Physical fusion	Dye disintegration (RhB)		[119]
100	MIL-125- NH_2	CDs	Ship–bottle	Dye disintegration (RhB)		[205]
101	MIL-100(Fe)	N-TiO_2 QDs	Physical fusion	Dye disintegration (MB/RhB)		[206]
102	Fe-MOFs	CdSe QDs	Bottle–ship	Degradation of RhB		[207]
103	ZIF-8	NDCQDs	Ship–bottle	Degradation of methylene blue		[208]
104	Eu-MOFs	CdTe QDs	Bottle–ship	Solar cell	Energy storage	[111]
105	Ni-MOFs	Co_9S_8 QDs	Intercalation	Supercapacitor		[118]
106	ZIF-8	ZnO QDs	Co-electrospinning followed by carbonization	Supercapacitor		[209]
107	ZIF-8	Nb_2O_5 QDs	Carbonization followed by hydrothermal treatment	Supercapacitor		[210]
108	ZIF-8	GQDs	Bottle–ship	Lithium-ion battery		[211]
109	ZIF-8	ZnO QDs	Physical fusion	Lithium-ion battery		[212]
110	UiO-66	SnO_x QDs	Ship–bottle	Lithium-ion battery		[213]
112	MOF-5	Ag_2S QDs	Physical fusion	Lithium-ion battery		[214]
113	Mo-MOFs	$MoSe_2$-MoO_3 QDs	Thermal induction	Sodium-ion battery		[215]
114	ZIF-8	VN QDs	Ship–bottle	Li–S batteries		[104]
115	ZIF-8	CDs	Bottle–ship	Light-emitting diodes	Opto-electronics	[216]
116	Zr-MOFs	CDs	Physical fusion with a binding agent	Light-emitting diodes		[123]
117	Cd-MOFs	CdTe QDs	Direct surface functionalization	Light-emitting diodes		[117]
118	ZIF-8	$CdSe_xS_{1-x}$/ZnS QDs	Ship–bottle	Light-emitting diodes		[217]
119	ZIF-8	$CsPbX_3$ QDs	Ship–bottle	Light-emitting diodes		[101]
120	EuW-MOFs	CDs	Bottle–ship	Multiluminescent materials		[218]
121	IRMOF-3	CdSe/CdS/ZnS QDs	Physical fusion	Photoluminescence		[219]
122	Cu-MOFs	Cu_2SnS_3 QDs	Bi-sacrificial templates	Nonlinear optics		[220]

used a thermal injection to combine UiO-67 and $CsPbX_3$ QDs precursors to generate $CsPbX_3$@UiO-67 at high temperatures (Figure 3b). A double-solvent technique has been successfully devised to avoid QDs' aggregation on the exterior surface of MOFs. By using this technique, QDs precursors, which have smaller sizes than MOF pores,

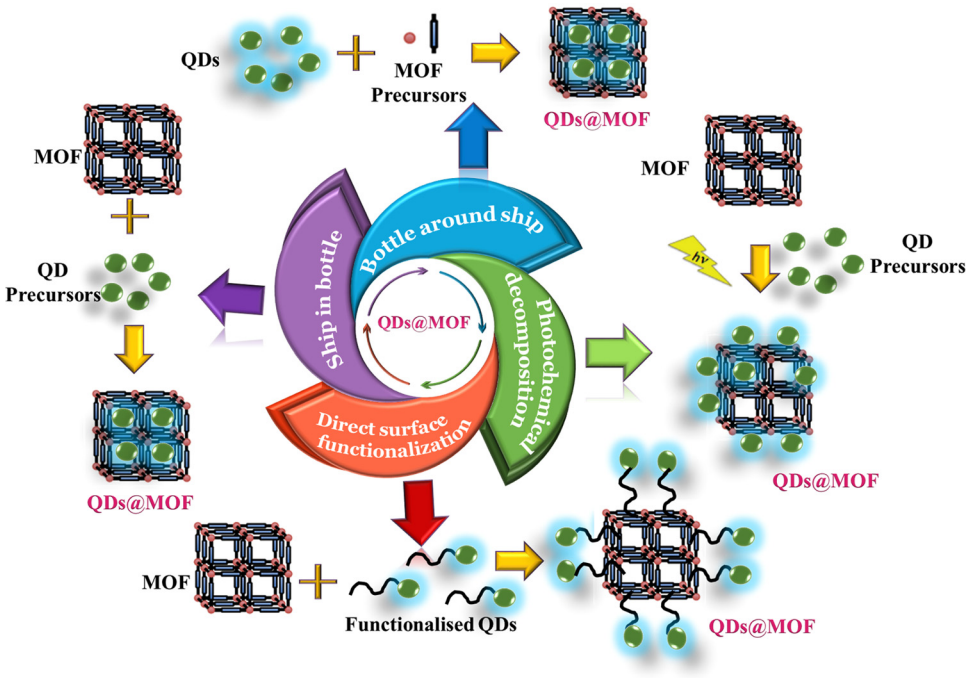

Figure 2: Schematic representation of various approaches deployed for the preparation of QDs@MOF.

passed into the hydrophilic cavities of MOFs *via* capillary action and hydrophilic contact, thus reducing the amount of QDs deposited on the exterior part of MOF. In this context, Meng and colleagues [110] used a twofold solution approach whereby a small amount of glucose (G) and CdS QD precursor solution were co-infiltrated into the cavity of MIL-101, which resulted in the formation of G/CdS@MIL-101, further subjected to calcination at 200°C to obtain the ultimate product carbon nanodots (CDs)/CdS@MIL-101.

It is worth noting that ship–bottle preparation procedures frequently rely on very extreme reaction conditions, such as elevated temperature and redox state, which might result in local network deterioration. This could also reduce the surface area of the MOF matrix, thus having a significant influence on applications that need porosity. However, the most significant advantage of this technology is to enable the creation of conformal MOF layers around QDs, which is a unique and demanding operation.

2.2 Bottle–ship

The bottle–ship strategy (Figure 2) is commonly known as the model synthesis methodology for QDs@MOF preparation. Following this method, QDs are initially produced and spread in a solvent-based stabilizer, such as a surfactant, to avoid agglomeration. Following that, MOF precursors are added to the solvent, which initiates MOF development around the QDs. During this process, organic linkages form divalent connections with capping moieties on the surface of the QDs. In this context, to develop a CdTe/Eu-MOF composite, Kaur *et al.* [111] employed CdTe QDs capped with cysteamine that were introduced to the Eu-MOF precursor solution, resulting in an ordered distribution of CdTe QDs in the Eu-MOF environment due to the interaction between the –COOH moieties of Eu-MOF and the $-NH_2$ groups on the exterior section of the CdTe QDs. Similarly, Mo *et al.* [112] followed the same methodology and prepared Fe(III)-MIL-88B-NH_2@ZnSeQDs for antigen detection where the solution of a MOF precursor and ZnSe QDs were heated at 100°C (for 20 h) in a Teflon-lined reactor. The ultimate desired compound was obtained by subsequent cooling followed by centrifugation (Figure 3c). Furthermore, Wang *et al.* [113] employed a capped polyvinyl pyrrolidone agent, which not only maintained the firmness and distribution of the particles but also stimulated the formation of ZIF-8 on the surface, thus establishing an intimate heterogeneous assembly between them. Importantly, this method successfully lowers the quantity of the QDs accumulated on the exterior part of the MOFs by avoiding the diffusion impedance of the nanoparticles infiltrating into the environment of the MOFs. Furthermore, because nanoparticles may be agglomerated prior to the assembly of frameworks, the shape and dimension of QDs can be tailored for specific applications.

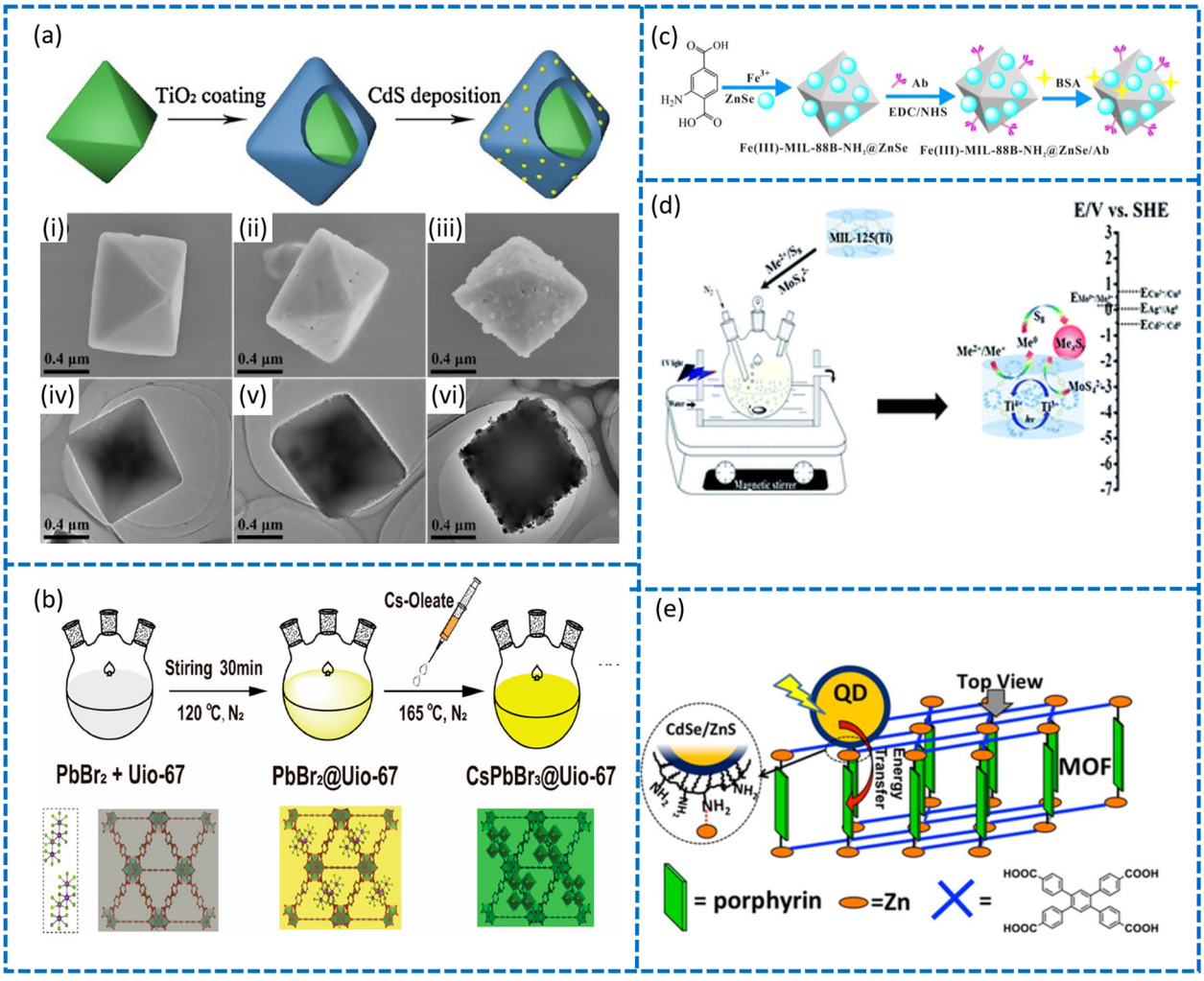

Figure 3: (a) Graphical representation of the construction of CdS/NH_2-MIL-125@TiO_2 and corresponding SEM and TEM images [107]. (b) Designed fabrication strategy for $CsPbBr_3$@Uio-67 composite formulation and accompanying structural diagrams [109]. (c) Synthesis scheme for CdS/NH_2-MIL-125@TiO_2 and antibody detection [112]. (d) Diagrammatic representation of the mechanism for photodeposition of Me_xS_y on MIL-125(Ti) [114]. (e) Illustrative representation of porphyrin-established MOFs with CdSe/ZnS core/shell QDs [116].

Unlike the ship–bottle and bottle–ship techniques, in which QDs were embedded in MOFs, the "photochemical-deposition" technique (Figure 2) involves depositing QDs on the exterior part of MOFs.

2.3 Photochemical deposition

The in situ synthesis and admission of QD particles into the exterior part of a MOF is aided by light in this method; photo-reduction of metallic precursors with a sufficient redox potential induces the production of QDs on the MOF surface. Direct binding with an appropriate linking group can be used to modify the surface area of MOFs with QDs. Utilizing this approach, Wang's group [114] used UV light to create hybrid materials of MIL-125(Ti) accumulated by CdS, CuS, and Ag_2S QDs. The mechanism of the photodeposition of Me_xS_y on MIL-125(Ti) is shown in Figure 3d. Similarly, Lin *et al.* [115] prepared a three-component hybrid material denoted as UiO-66/CdS/1% reduced graphene oxide, following the above-described method, and acquired significant results toward photocatalytic applications. The key drawbacks of this technology include two critical procedures to synthesize QD-MOF composites: first, it is the in situ synthesis and distribution of QDs on the interface of MOFs and, second, the adequate photoreduction potential to convert QD precursors to QDs, which might be tough at times.

2.4 Direct surface functionalization

Direct surface functionalization (Figure 2) is another tactic to suspend QDs on the interface of MOFs. The surface ligands of QDs are sequentially replaced with an appropriate capping group, which can establish direct interaction with MOF particles either by coordinative interaction or by some nonspecific contacts. The primary distinction between this strategy and the three preceding ones is that both MOFs and QDs are pre-designed prior to being assembled. Moreover, the key benefit of this type of synthesis includes the easy regulation of the form and size of QDs, as well as the construction of MOFs. To prepare porphyrin-based MOFs, Jin *et al.* [116] followed the abovementioned method and developed porphyrin-based MOFs with CdSe/ZnS QDs where the amino-functionalized QDs firmly adhered to the surface of the MOFs through zinc metal (Figure 3e). Similarly, employing the same strategies, Mondal *et al.* [117] prepared an MOF-functionalized cysteine-capped CdTe QDs, which functioned as a proficient white light-emitting phosphor material for display applications. In contrast to the previous three approaches, in this method, MOFs and QDs are pre-formed before being assembled. This approach has the advantage of enabling to control the shape and size of QDs as well as the morphology of MOFs.

2.5 Other synthesis methodologies

In addition, some other methods, such as intercalation [118], physical fusion [74,119] drop casting [120], and electrochemical depositions [121,122], have been developed for the preparation of QDs@MOF composites. The "physical mixing" approach is more simple and may be divided into two categories. The first one involves the use of physical force binding to combine QDs with MOFs, and the second one employs ultrasonic fusion. Utilizing the above-cited methods, Wang *et al.* [123] fabricated white light-emitting phosphor materials using carbon dots (CDs) and a Zr(IV)-MOF by physical fusion with a binding agent. Another extensively used technique is electrochemical deposition, which involves dispersing QDs in an electrolyte and depositing them on the interface of MOFs using an electric current. Recently, Chen *et al.* [106] adopted a slightly different tactic for the synthesis of UiO-66-NH_2/black phosphorus QDs (MOF/BPQDs). The in situ synthesis of the composite was carried out on the carboxyl cellulose nanofiber (CNF) surface, which served as nucleation centers due to the presence of abundant carboxyl groups. The CNF aerogel shows high structural adaptability and little MOF erosion in BP@CNF-MOF, which demonstrates the reciprocal physical contact and involvement of CNFs, along with excellent binding affinities among MOF crystals and the CNF aerogel. According to the aforementioned methodologies, the techniques of embedding QDs within MOF matrixes are more effective than seeding MOF crystals with QDs. Not only does the encapsulation of QDs inside MOFs prevent QDs from covering MOFs, but it also inhibits QDs from clustering. In addition, after being encapsulated by MOFs, the robustness of QDs increases.

3 Application of QDs@MOFs

As a new functional hybrid material, QDs@MOFs hold greater stability, robust adsorption capacity, and unique intriguing properties, which make them ideal candidates for numerous applications. The applicability of QDs@MOFs in different fields (Figure 4), such as sensing, bio-imaging, energy generation, and energy storage, is detailed in this section and the applications of these new fields of interest are presented in Table 1.

3.1 Sensing

Sensors can help to improve the quality of life by aiding in medical diagnosis, increasing the efficiency of renewable resources, such as fuel cells and batteries, photovoltaics, pollution management, enhanced health, welfare, and security for people. Recently, QDs@MOFs have been considered attractive materials for fabricating different fluorescence sensors due to their high quantum yields, extended lives, outstanding photo-stability, and size-dependent emission wavelengths.

3.1.1 Metal ion detection

With the industrial growth, a large number of metal ions, for example, Pb^{2+}, Fe^{3+}, Cr^{2+}, Cu^{2+}, and Hg^{2+}, have been discharged into water, destroying the water environment and posing a threat to human safety. As a result, the advancement of an effective metal ion detection technology is a precondition for heavy metal pollution prevention and management. Because of its high level of sensitivity, low detection limit, strong selectivity, broad detection array, quick response, decent anti-jamming capability, and simplicity of maneuver, metal ion detection

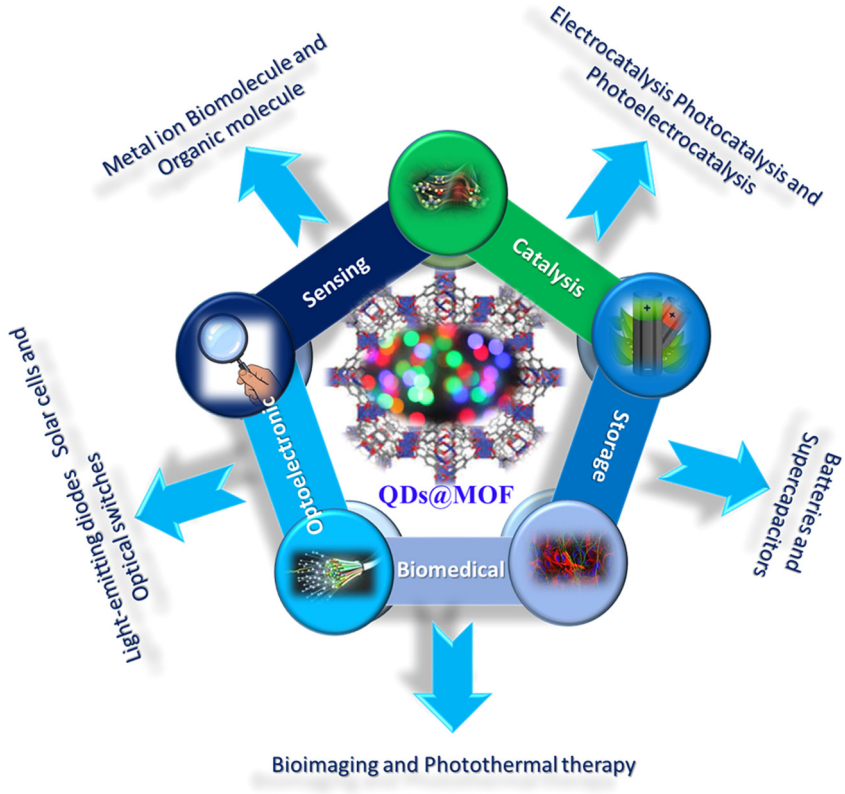

Figure 4: A schematic representation of QDs@MOF for various captivating applications.

using fluorescence-based QD biological sensors has recently drawn a lot of attention. For instance, Chen *et al.* [114] employed UiO-66-NH_2/black phosphorus QDs (MOF/BPQDs) adorned on the CNF aerogel for uranium extraction from seawater (Figure 5a). The creation of a heterojunction between BPQDs and UiO-66-NH_2 displays outstanding photocatalytic activity (Figure 5b), which efficiently kills marine bacteria by releasing a huge amount of reactive oxygen species. Similarly, to design a ratiometric fluorescence device for the recognition of Cr, Wang *et al.* [124] rationally developed CDs@Eu-MOFs (Figure 5c). Surprisingly, the synthesized CDs@Eu-MOFs outperform Cr(VI) in terms of excellent selectivity (Figure 5d(i)) in the presence of a wide range of metal ions (Na^+, K^+, Zn^{2+}, Pb^{2+}, NH_4^+, Mn^{2+}, Mg^{2+}, Fe^{2+}, Co^{2+}, Ca^{2+}, Cu^{2+}, Fe^{3+}, Hg^{2+}, Al^{3+} $Cr_2O_7^{2-}$) with potentiometric detection of Cr(VI) under optimal circumstances, with a linear range of 2–100 μM and a low detection limit (LOD) of 0.21 μM (Figure 5d(ii)).

3.1.2 Detection of biomolecules

Direct identification of biological systems, for example, an enzyme or an antigen, by means of a QDs@MOF probe should be more inventive for biological intuiting applications. Several studies have been conducted so far using QDs@MOFs for the detection of biomolecules. For example, Wang *et al.* [125] developed a CdTe QDs@ZIF-365 as a bi-functional ratiometric probe for highly subtle recognition of L-histidine and Cu^{2+} by adopting the post-synthesis strategy (Figure 6a). The experimental findings revealed that the CdTe QDs@ZIF-365 can be employed as an outstanding photo-luminescent probe for L-histidine and Cu^{2+} with a steep K_{sv} (6.0507×10^8 [M^{-1}] and 2.7417×10^7 [M^{-1}]) value and low detection (Figure 6a). Similarly, Xie *et al.* [126] recently implemented LMOFs (luminous metal–organic frameworks) -CDs@ZIF-8 by incorporating blue-emitting CDs into ZIF-8 and employed it as a fluorescent sensor for highly sensitive and discerning recognition of dopamine (DA) (Figure 6b). The sustained pores in ZIF-8 not only provide free space for analytes but they may also selectively collect and intensify DA molecules through interactions between the analyte DA and the functional site of the framework. Furthermore, CDs can be used as signal probes to convert chemical signals from CD-analyte interactions into fluorescent signals. When compared to CDs, the CDs@ZIF-8 creates a novel sensing platform. As a result, the CDs@ZIF-8-based recognition technique for

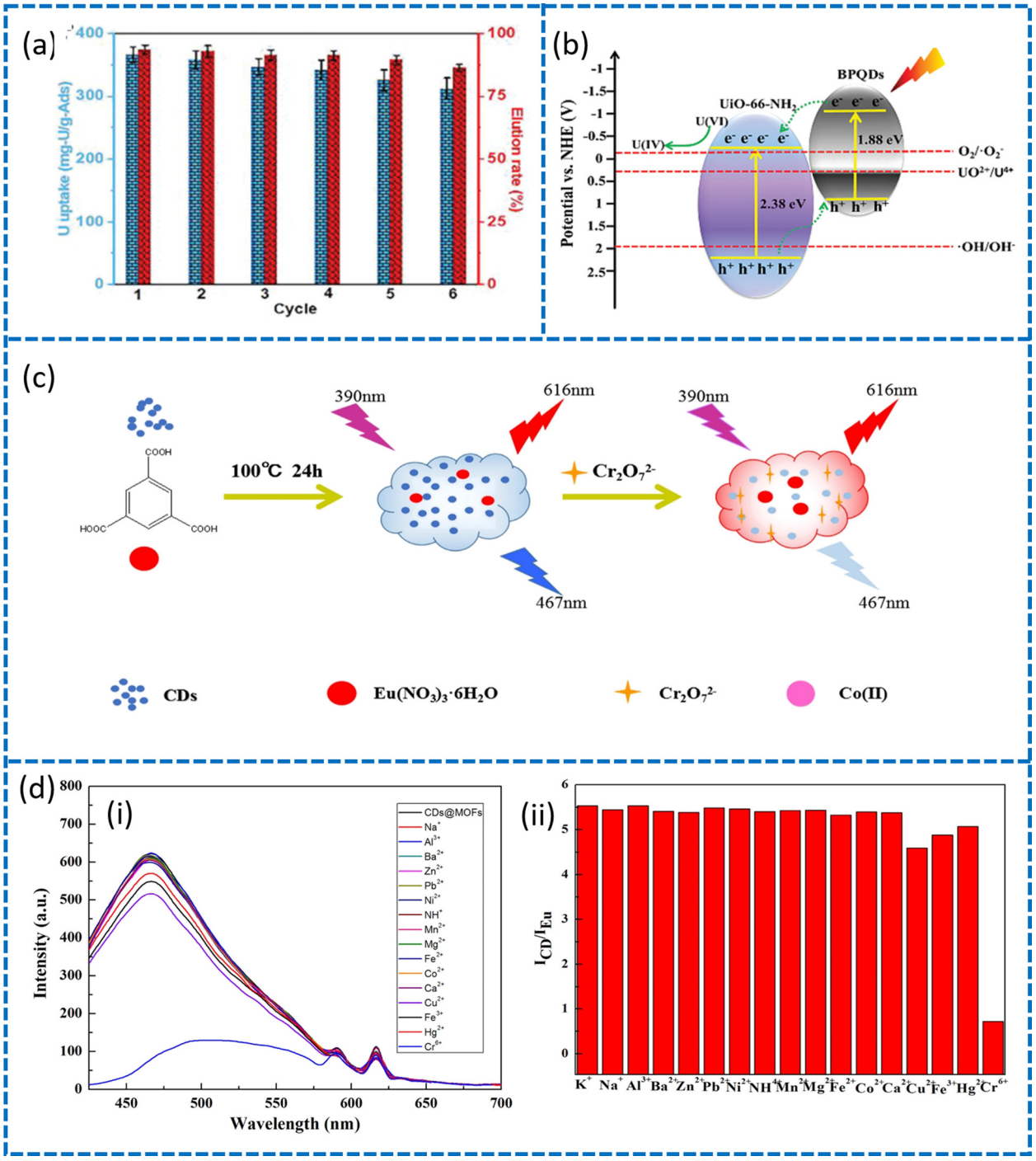

Figure 5: (a) Under light irradiation, uranium adsorption capacity and elution efficiency in six consecutive cycles. (b) A schematic representation of the photocatalytic reduction of U(VI) utilizing MOF/BPQDs hybrid under solar-light irradiation [106]. (c) A schematic representation of the photocatalytic reduction of U(VI) utilizing MOF/BPQDs hybrid under solar-light irradiation. (d) The CDs@Eu-MOFs fluorescence selectivity spectra in the absence and presence of different metal ions [124].

DA was shown to have a large concentration dynamic (0.1–200 M) and an LOD of 16.64 nM (Figure 6b and c). According to the findings, the produced QDs@MOF might be ideal probes for detecting cell biological properties and could be utilized as cell strength monitors and bio-probes.

3.1.3 Recognition of other entities

QDs@MOFs have been investigated for the recognition of other materials. For example, Zhou *et al.* [127] developed a robust ultra-sensitive electrochemiluminescence sensor

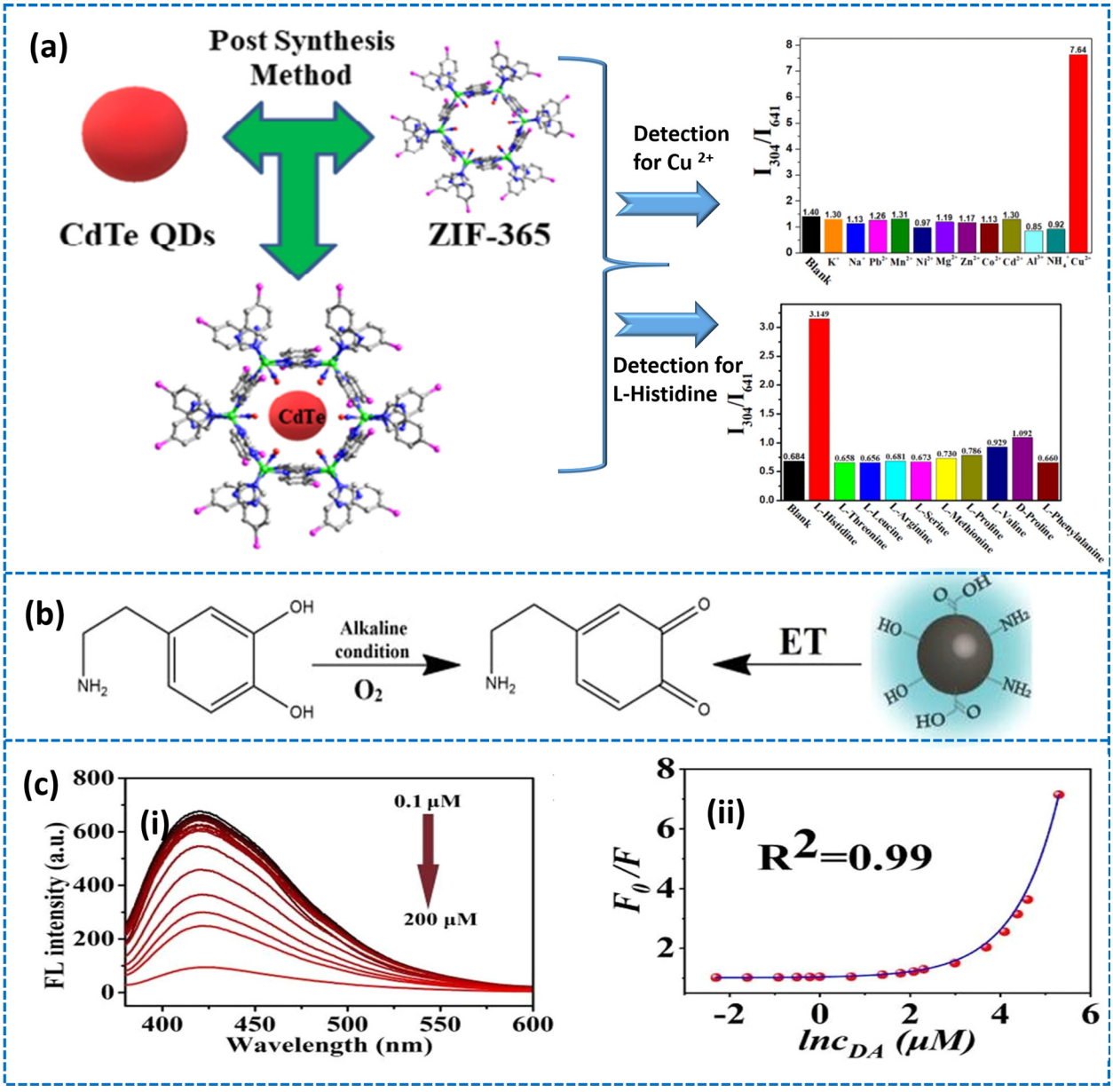

Figure 6: (a) The illustrative representation of fabrication of a CdTe QDs@ZIF-365 ratiometric fluorescence probe and its use for very delicate recognition of L-histidine and Cu^{2+} [125]; (b) diagrammatic representation of detection of DA through a possible mechanism. (c) FL emission bands of CDs@ZIF-8, with different DA concentrations [126].

(CDs@HKUST-1) for the recognition of catechol. The results revealed that the definite surface area of HKUST-1 on CDs might significantly increase the sensor's sensitivity. The as-synthesized sensor showed a varied linear range of 5.0109–2.5105 mol L^{-1} under ideal circumstances, with an LOD of 3.8109 mol L^{-1} ($S/N = 3$). Employing a post-synthetic modification method, Yang *et al.* [128] discovered an amine-CQDs@UiO-66 fluorescence probe by using amine-functionalized carbon QDs (amine-CQDs) in combination with UiO-66. In this investigation, UiO-66 was employed as an adsorbent to selectively collect and augment the target compounds. Here, the amine-CQDs were used as a template molecule to evaluate the connection between UiO-66 and the target compounds in a specific fashion and to subsequently convert these chemical reactions into recognizable fluorescence signals. As a result, QDs@MOFs provide a novel approach to creating hybrids with synergistic characteristics, fluorescence, and excellent durability for various sensing applications.

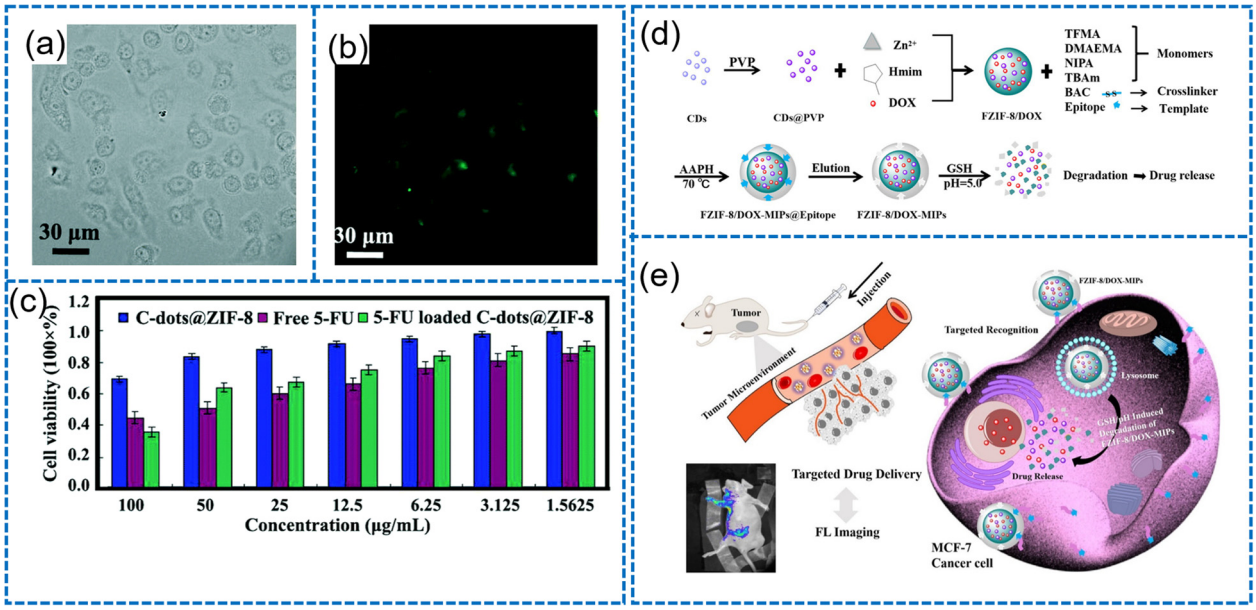

Figure 7: (a) The picture of differential interference contrast. (b) Adopted 5-FU-encumbered C-dots@ZIF-8 with spot-like green fluorescence. (c) Cytotoxicity toward Hela cells *in vitro* [129]. (d) FZIF-8/DOX-MIP production and GSH/pH route of twofold stimulation and decay. (e) Graphical representation of tailored imaging and GSH/pH-receptive drug transport of FZIF-8/DOX-MIPs [130].

3.2 Biomedical

The unusual features (excellent biocompatibility, bioavailability, and renewability) of QDs@MOFs have attracted a lot of interest in the biomedical profession in recent years because, among other applications, they can be used for real-time tissue imaging (bioimaging), diagnostics, single-molecule probes, and medication administration. Herein, we have concentrated on two major biomedical applications: bioimaging and photothermal therapy.

3.2.1 Bioimaging

Bioimaging is a useful research strategy in contemporary biology and medicine that may quickly and easily offer clear and understandable biological information. Several investigations have shown that QDs@MOFs have great bioimaging capabilities due to their PL characteristics. For the first time, He *et al.* [129] used a straightforward two-step technique to create CDs and ZIF-8-based nanocomposites. The coordination contacts between Zn^{2+} ions and functional groups (–COOH/–N) on the CDs were reinforced to encase the CDs on the ZIF-8. The resulting CDs@ZIF-8 showed green fluorescence as well as being an excellent pH-receptive anti-cancer drug carrier and cell imaging (Figure 7a and b). According to *in vitro* cell studies, it has been corroborated that the nanocomposites exhibited excellent cyto-compatibility and could be endocytosed through cells for cell imaging and drug administration (Figure 7c). Furthermore, Qin and coworkers [130] recently developed a biodegradable nano-platform of molecularly imprinted polymer (MIP)-alleviated fluorescent ZIF-8 loaded with doxorubicin (DOX), (FZIF-8/DOX-MIPs) for drug delivery and imaging in a glutathione (GSH)/pH multi-stimulation system (Figure 7d and e). It is worth mentioning that CDs generate bright red fluorescence, allowing more precise tumor cell imaging. With time, the fluorescent gesture of FZIF-8/DOX-MIPs grew in the tumor location of mice. Furthermore, in an acidic tumor environment, the biological degradation of ZIF-8 and MIPs was favorable for drug release.

3.2.2 Photothermal therapy

Photothermal treatment (PTT) using near-infrared (NIR) light for tumor hyperthermia ablation has been intensively explored in recent years and has sparked a lot of interest. PTT has fewer adverse effects than standard tumor treatment techniques because local heat may be properly regulated in temporal and spatial lobes. MOFs and other two-dimensional (2D) materials have recently been investigated as photodynamic agents (PTAs) for PTT applications *in vitro* and *in vivo*. When three-dimensional (3D) MOFs are converted into 2D sheets, the resulting

MOF sheets may absorb a huge quantity of guest molecules *via* a noncovalent contact. Nevertheless, the poor photothermal renovation efficacy (PTCE) of 2D materials, as well as their considerable dimensional size, limits their practical application in PTT. As a result, there is a significant need for ultra-small PTAs with immense PTCE to attain a remarkable competence in photothermal tumor therapy. QDs@MOF materials, on the other hand, provide a suitable space for loading QDs and avoiding QD aggregation due to their large specific surface area and ordered pores. Furthermore, QDs help MOFs to acquire better physicochemical properties. The close heterojunction or interfacial contact between QDs and MOFs speeds up the transfer of electrons and efficiently prevents the recombination of photo-generated charges. In addition, the developed QDs@MOFs might be suitable PTAs because of their outstanding NIR adsorption and biocompatibility characteristics. For example, Liu *et al.* [131] employed an MOF hybridized with black phosphorus QDs (BPQDS) as a tandem catalyst to improve the treatment of hypoxic tumor cells (Figure 8a). The integrated MOF system was able to alter H_2O_2 to O_2 in the MOF-alleviated catalase superficial layer, and then, O_2 was introduced unswervingly into the MOF-sensitized BQ central, resulting in an excellent quantum yield of singlet oxygen. Remarkably, without catalase, the MOF system's photodynamic treatment efficacy was 8.7 times higher after internalization, indicating an improved therapeutic impact besides hypoxic tumor cells (Figure 8b).

These findings imply that QDs@MOFs will usher in a new era of tumor PTT. Tian *et al.* [132] employed a very simple one-pot technique to formulate a versatile manifesto for a symbiotic chemo- and photothermal therapy. They utilized ZIF-8 as drug nanocarriers where the implanted GQDs functioned as indigenous photothermal kernels (Figure 8c). When DOX was exploited, a prototypical anticancer drug, the findings revealed that the monodisperse ZIF-8/GQDs (size 500–1,000 Å) were able to capture DOX throughout the manufacturing phase and activate DOX discharge under acidic circumstances. The DOX-loaded ZIF-8/GQDs were able to readily transform NIR illumination into heat and, therefore, raise the temperature. When breast cancer 4T1 cells were used as a prototype biological system, the findings confirmed that combining chemo-thermal treatment and PTT with DOX-ZIF-8/GQDs had a substantial harmonious impact, leading to greater performance in killing cancer cells than the photothermal therapy and chemotherapy alone

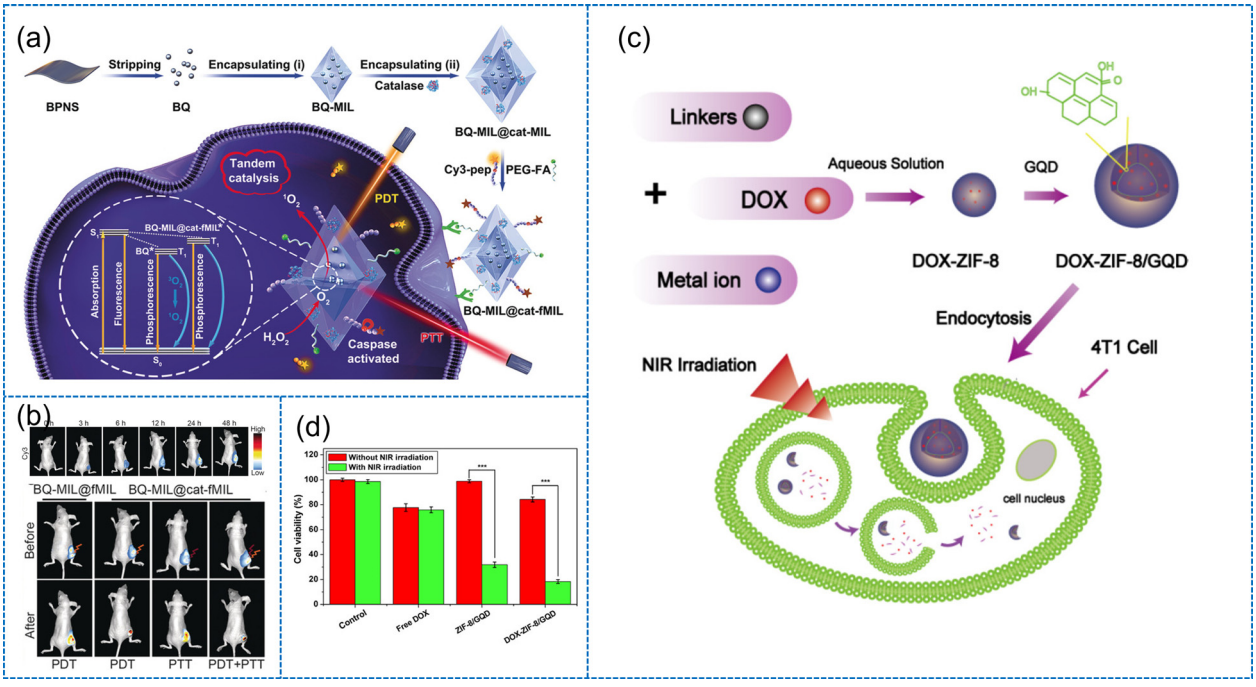

Figure 8: (a) Stepwise construction of BQ-hybridized MOF catalyst and action toward hypoxic tumor cell treatment. (b) After being inoculated with BQ-MIL@cat-fMIL, time-dependent *in vivo* fluorescence images of a mouse carrying a subcutaneous HeLa tumor and after injection of BQ-MIL@cat-fMIL or BQ-MIL@fMIL *in vivo* fluorescence imaging evaluated the treatment upshot on mice malignant cells [131]. (c) Schematic representation of the development of ZIF-8/GQDs with the recapitulation of DOX. (d) After 8 h of incubation, cell viability study of 4T1 cells with and without free DOX, ZIF-8/GQD, and DOX-ZIF-8/GQD suspensions and deprived of 3 min NIR radiation [132].

(Figure 8d). As a result, ZIF-8/GQDs might be useful as adaptable nanosystems in cancer treatment. These investigations revealed that QDs@MOFs have an extensive range of applications in biological and medical fields that are both benign and proficient.

3.3 Catalysis

Recently, tremendous progress has been achieved in the improvement of MOF-based QD materials as high competence catalysts/co-catalysts in catalysis systems, including GQDs, CDs, Se QDs, and Mxene QDs. In this context, QDs@MOFs are considered a promising catalyst/co-catalyst due to their tenability nature and robustness.

3.3.1 Electrocatalysis

Electrocatalysis is a highly advanced oxidation process (AOP) that has been extensively investigated in energy and conservational applications, such as the hydrogen reduction reaction, nitrogen reduction reaction (NRR), hydrogen evolution reaction (HER), methanol oxidation reaction, oxygen reduction reaction (ORR), and oxygen evolution reaction (OER). Among renewable-energy technologies, electrocatalytic applications are becoming highly indispensable. As a result of their outstanding characteristics, QDs@MOFs might play a significant part in the electrocatalytic processes. Despite the fact that many investigations have focused so far on the use of QDs in electrocatalysis, exploration of QDs@MOFs in electrocatalysis has just freshly come to the forefront. Zhou *et al.* [180] tested a unique MOF catalyst, CdS@PCN-224(Ni), and utilized it for HER in an acidic environment. The findings revealed a prodigious electrocatalytic performance with a Tafel slope of ~91 mV dec^{-1}, an overpotential of 120 mV, and a current density of 10 mA cm^{-2}, which is nearly identical to the Pt/C (~43 mV dec^{-1}). CdS@PCN-224(Ni) has a double-layer capacitance (Cdl) of 9.75 mF cm^{-2}, which is significantly higher than PCN-224 (2.33 mF cm^{-2}) (Figure 9a and b). Similarly, fuel cells have been actively investigated among various energy conversion technologies because of their lower pollution levels, superior energy transformation proficiency, and fuel diversity. The oxygen reduction process, however, is significantly limiting the overall reaction efficiency of the fuel cells due to their essentially slow kinetics. In this context, Ye *et al.* [192] reported a new and simple approach for manufacturing ZIF-derived Co–N–C ORR catalysts by carefully regulating the rate of crystallization of ZIFs. The experimental evidence showed that in an alkaline medium, the Co–N–C catalyst has a high ORR activity ($E_{1/2}$ of 0.9 V), which can compete with commercial Pt/C ($E_{1/2}$ of 0.83 V) (Figure 9c and d). Similarly, a bifunctional electrocatalyst was prepared by Ye *et al.* [59] using a simple hydrothermal technique. Such highly permeable cuboids of Pt QDs@Fe-MOF material demonstrated excellent electrocatalytic activity toward HER, OER, and overall water splitting. Interestingly, in 1 M KOH, the electrocatalyst with exceptionally low Pt QD content (1.85 μg cm^{-2}) only required an overpotential of 191 and 33 mV, respectively, to achieve a current density of 100 and 10 mA cm^{-2}. Furthermore, the Pt QDs@Fe-MOF/NF (Ni foam) electrodes had exceptional potency, delivering a current density of 10 mA cm^{-2} at 1.47 V during at least 100 h of water splitting. These findings suggest that QDs@MOFs show promising potential in the realm of electrocatalysis; however, additional studies are warranted.

3.3.2 Photocatalysis

Another proficient AOP, photocatalysis, has been extensively investigated and seems extremely promising for dealing with global energy and environmental concerns. In this context, QDs@MOFs are viewed as potential visible-light catalysts for assorted systems, namely photocatalytic CO_2 reduction, H_2 production, H_2 reduction, pollutant degradation, and other applications in this domain. As an example, Liu *et al.* [186] illustrated the integration of GQDs on MIL-101(Fe) to create GQD/MIL-101(Fe)(G/M101) by employing a one-step solvothermal technique. With the use of MIL-101(Fe) and GQD sensitization, the photocatalytic reduction efficiency of CO_2 to generate CO could be considerably improved. Experimental evidence revealed that the rate of CO generation over G/M101-5% (224.71 μmol h^{-1} g^{-1}) is five times greater in comparison with MIL-101(Fe) (46.2 μmol h^{-1} g^{-1}) (Figure 10a and b). Furthermore, photocatalytic nitrogen fixation is regarded as a potential strategy for obtaining high NH_3 production, which is critical for human growth and industrial advancement. Nevertheless, because of the inert nature of nitrogen, it is important to investigate superior competence catalysts for nitrogen reduction. In this context, Qin *et al.* [191] used MXene QDs (Ti_3C_2-QDs) and a 2D nickel metalorganic framework (Ni-MOF), following a self-assembly approach, to increase the photocatalytic proficiency of the N_2 reduction process. The optimum Ti_3C_2-QDs/Ni-MOF heterostructure produced a significant amount of ammonia (88.79 μmol g_{cat}^{-1} h^{-1}) (Figure 10c). These findings provide space for further applications of QDs@MOF in photocatalysis.

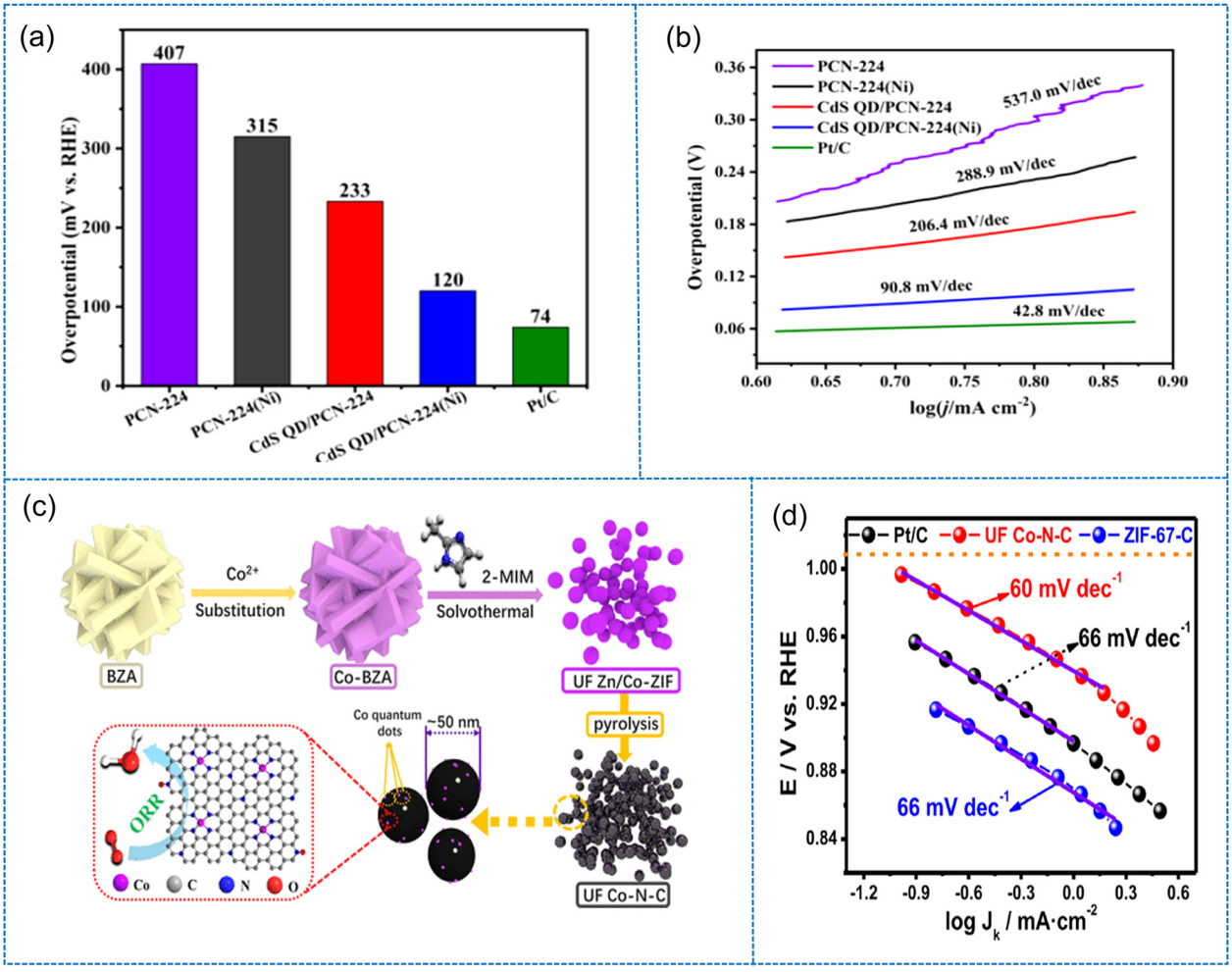

Figure 9: (a) Overpotential of PCN-224, PCN-224(Ni), CdS@PCN-224, CdS@PCN-224(Ni), and Pt/C electrodes at the current density of 10 mA cm^{-3}. (b) Tafel plots of PCN-224, PCN-224(Ni), CdS@PCN-224, CdS@PCN-224(Ni) and Pt/C [180]. (c) Illustrative representation of the imitation process of UF Co–N–C. (d) ORR efficiency in O_2-saturated environment 0.1 M KOH electrolyte [192].

3.3.3 Photoelectrocatalysis (PEC)

PEC is a potent technology that combines heterogeneous photocatalysis with electrochemical methods. Extensive research has been conducted so far on the use of QDs@MOFs in PEC for water splitting. As a result of their unique characteristics, QDs@MOFs may have great application potential in PEC. Shi *et al.* [221] suggested that MOF-derived TiO_2 can be used to boost the productivity of a TiO_2-QDs established PEC system for hydrogen evolution. When compared to conventional TiO_2 films, an MOF-impregnated TiO_2 film stimulated by core–shell CdSe@CdS QDs demonstrated a +42.1% increase in the PEC device stability and a +47.6% increase in the PEC performance. The inclusion of mixed rutile/anatase phases enhances the performance by creating a promising band energy arrangement for the dissociation of photogenerated charges. Even though there are only a few studies on PEC with QDs@MOF-based materials, this approach is intriguing and should be given greater attention. These findings pave the way for QDs@MOFs being used in photocatalysis in the future.

3.4 Energy storage

In this twenty-first decade, increasing energy consumption, the depletion of fossil fuels, and growing concerns about industrial pollution have stimulated the improvement of eco-friendly technologies to create new alternative and renewable energy resources. In this context, QDs@MOFs are regarded as viable catalytic systems for energy storage devices because of their unique chemical, physical, and electrical features.

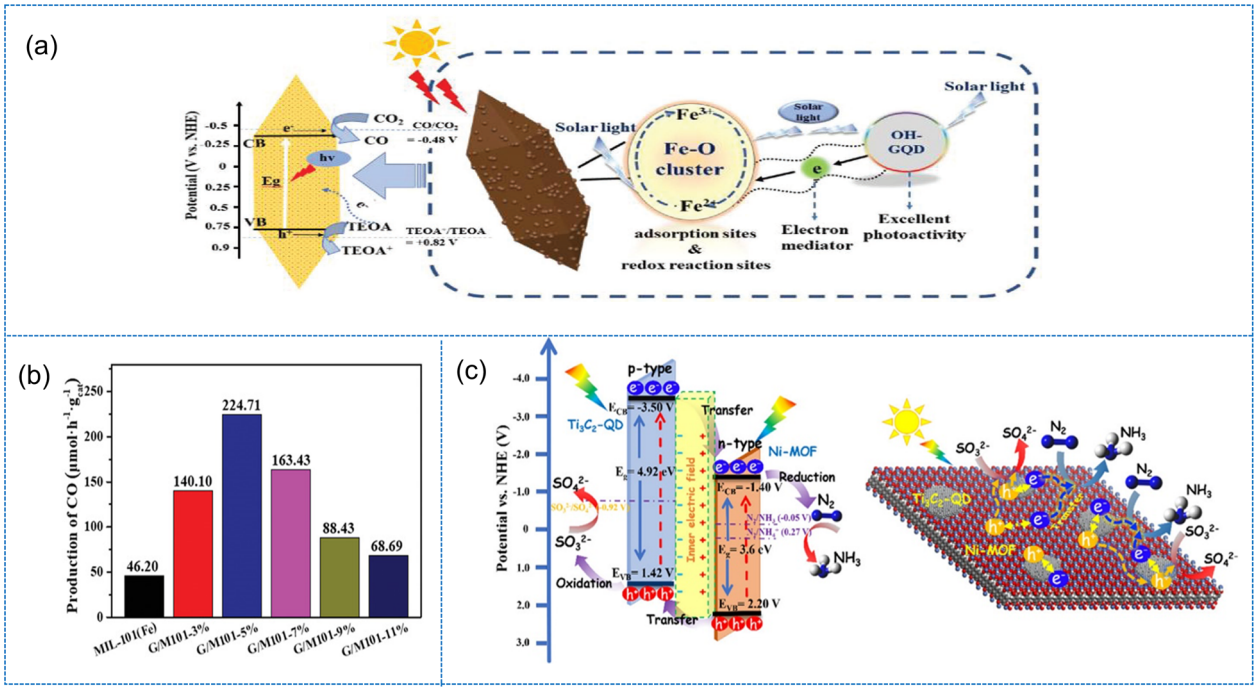

Figure 10: (a) Schematic representation for visible light-assisted reduction of CO_2 over G/M101 nanocomposite. (b) Photocatalytic CO production by GQDs/MIL-101(Fe) [186]. (c) Diagrammatic representation of energy band positions, localized charge separation, and movement through the photocatalytic N_2 reduction over Ti_3C_2-QDs/Ni-MOF [191].

3.4.1 Batteries

With the advancement of science and technology, a great deal of focus has been placed on creating next-generation electrochemical energy storage technologies (a few examples are batteries, supercapacitors, solar cells, *etc.*). Because of their environmental friendliness and great energy density, batteries are the most frequently investigated electrochemical energy storage devices.

QDs@MOF-based materials have shown considerable promise for battery applications in recent years due to their better theoretical Li storage capacity, advantageous electrical conductivity, truncated functional voltage range, low dispersal fences for Li mobility, and outstanding mechanical characteristics. For instance, Saroha *et al.* [104] recently prepared multilayer porous N-doped C nanofibers encompassing vanadium nitride QDs and MOF-based hollow N-doped C nanocages for improved lithium–sulfur batteries as functional interlayers. The experimental findings revealed that because of the high sulfur concentration (80 wt%) and loading (ca. 4 mg cm^{-2}) in the sulfur electrodes, the Li–S cell utilizing the novel nanostructured self-supporting interlayer displayed better rate proficiency and steady cycling recital (decay rate of 0.02%/cycle at 0.5 C). Interestingly, after 100 cycles of charging and discharging at 0.05 C, the Li–S cell provided a steady areal capacity of 5.0 mA h cm^{-2} despite an ultra-high sulfur loading of 11.0 mg cm^{-2} (Figure 11a–c). Zhang *et al.* [222] prepared ZIF-8/graphene oxide hybrids as anode materials for sodium-ion batteries. The capacity of the synthesized material was quite stable at 539 mA h g^{-1} at 100 mA g^{-1}, 512 mA h g^{-1} at 200 mA g^{-1}, and 456 mA h g^{-1} at 500 mA g^{-1} after 100 cycles. After 300 cycles, upon raising the current density to 1 A g^{-1}, the capacity still attained 362 mA g^{-1} (Figure 11d). This investigation revealed that QDs@MOF-based materials have the potential for developing high-performance electrode material in batteries.

3.4.2 Supercapacitors

A supercapacitor, like batteries, is an imperative energy storage equipment that has the potential to be used in electric vehicles and other portable devices because of its extraordinary power density, firm charging/discharging capabilities, and extended life cycle. Due to their structural flexibility, excellent electrical conductivity, hydrophilic surface, and high surface area, QDs@MOFs have been extensively researched. These intriguing features may result in ultra-high volumetric capacitance as they provide quick electron transfer pathways and a huge electrochemically energetic surface for a quick and reversible

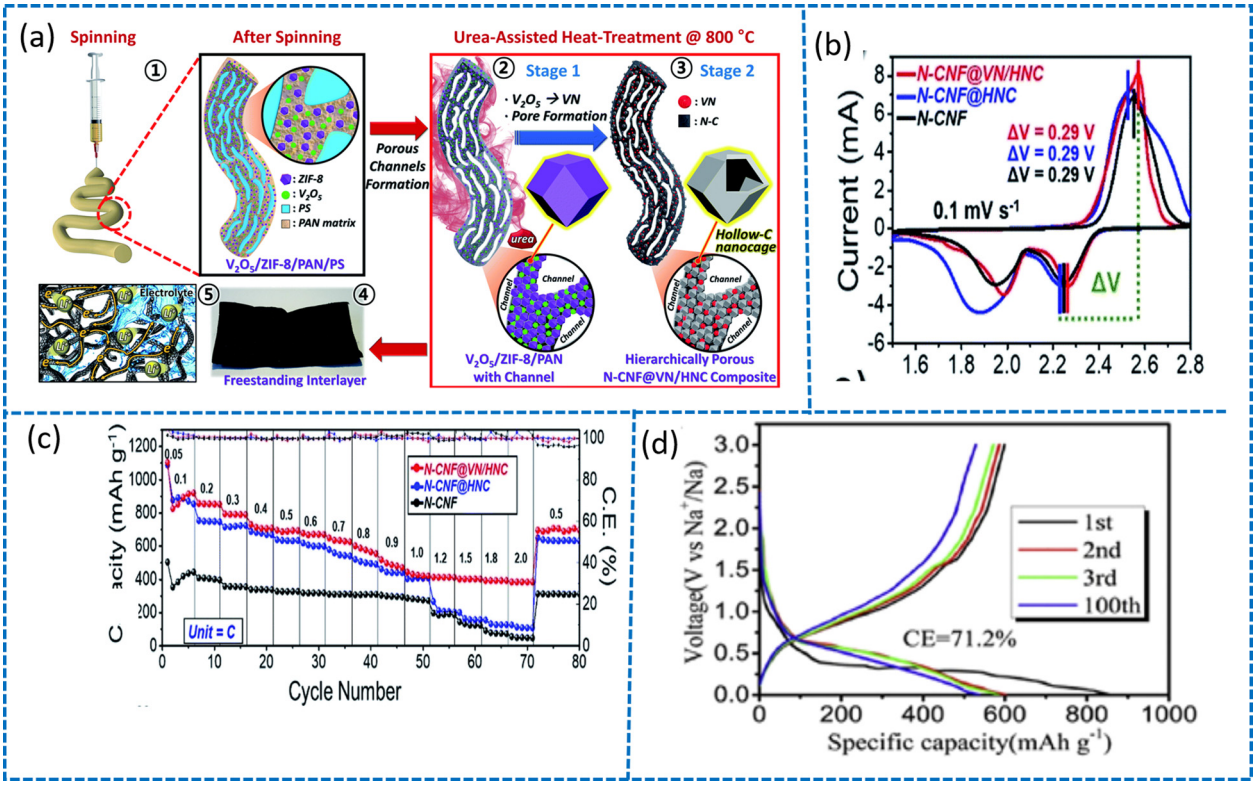

Figure 11: (a) Schematic illustration for the construction mechanism of N-CNF@VN/HNC. (b) Charge–discharge voltage profiles of (N-CNF@VN/HNC) at 0.05 C. (c) Rate capability analysis of (N-CNF@VN/HNC) at different C-rates [104]. (d) Galvanostatic charge/discharge profile (current density of 100 mA g^{-1}) [222].

faradaic reaction. Yang *et al.* [118] reported *in situ* formations of Co_9S_8 QDs in the interlayer of MOF-derived layered double hydroxide (LDH) nanoarrays for supercharged amalgamated supercapacitors. Remarkably, the selectively produced Co_9S_8-QDs displayed numerous active sites that enhanced the electrochemical characteristics, such as cyclic stability, capacitive performance, and electrical conductivity. Because of the mutually beneficial partnership, the composite material distributed an extremely high electrochemical capacity of 350.6 mA h g^{-1} (2,504 F g^{-1}) at 1 A g^{-1}. Moreover, blended supercapacitors produced with CF@NiCoZn-LDH/Co_9S_8-QDs and carbon nanosheets, enhanced by single-walled carbon nanotubes, had a remarkable energy density of 56.4 W h kg^{-1} at a power density of 875 W kg^{-1}, with a capacity retention of 95.3% after 8,000 charging and discharging cycles. (Figure 12a and b). Similarly, Liu *et al.* [210] prepared a hybrid material, NQD-NC, made up of Nb_2O_5 QDs implemented on nitrogen-doped porous carbon imitative from ZIF-8 dodecahedrons, which showed excellent electrochemical enactment including ultrahigh energy and power density (76.9 W h kg^{-1} and 11,250 W kg^{-1}, respectively) and longer cyclic firmness after 4,500 cycles with the retaining capacity of ~85% at 5 A g^{-1} in a voltage range of 0.5–3.0 V (Figure 12c and d). In this investigation, QDs@MOFs were shown to be potential options for developing extraordinary recital supercapacitor devices.

3.5 Optoelectronic devices

The core and most fundamental component of optoelectronic technology is optoelectronic devices, and as the technology advances, a wide range of optoelectronics, such as optical switches, white light-emitting diodes (W-LEDs), solar cells, and lasers, are developed. In the limited range of visible light, MOFs are recognized as excellent luminous materials, whereas QDs are considered a suitable candidate for the preparation of white light-emitting devices due to their broad absorption range, high extinction coefficient, and high quantum yield. Many MOF-imitative QDs, such as GQDs, CQDs, perovskite QDs, and Mxene QDs, have recently been demonstrated to have exceptional electron donors and acceptors in their photoexcited states, making them interesting for deployment in optoelectronics. For example, Wang *et al.* [123] developed, by combining CDs

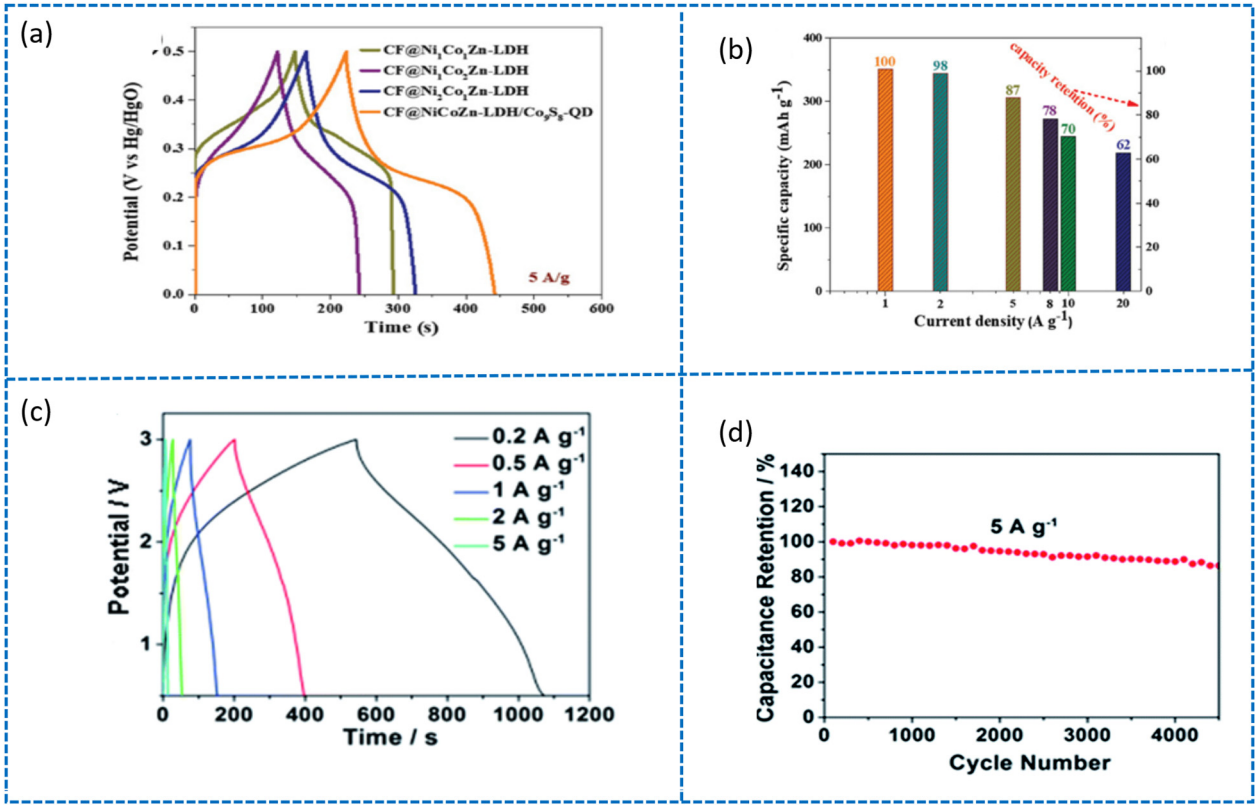

Figure 12: (a) Galvanostatic charge–discharge curves of $NixCo_3$–*x*Zn-LDH and CF@NiCoZn-LDH/Co_9S_8-QDs (current density of 5 A g^{-1}). (b) The specific capacity and capacity retention rate of CF@NiCoZn-LDH/Co_9S_8-QDs (current densities of 1–20 A g^{-1}) [118]. (c) AC/NQDs-NC HSC charge–discharge profiles (potential range of 0.5–3.0 V) at various current densities (0.2–5 A g^{-1}. (d) Cycle performance of NQDs-NC HSC for around 4,500 cycles (current density of 5 A g^{-1}) [210].

with Zr(IV)-MOFs, a novel rare-earth free material that emits white light when excited at 365 nm, with a PL quantum yield of 37% in the solid state (Figure 13a). A CIE chromaticity coordinate of (0.31, 0.34) (Figure 13b and c), a luminous efficiency of 1.7 lm W^{-1}, and a high color-rendering index (CRI) of 82 were achieved by dropping the CDs/Zr-MOF on a marketable UV LED chip.

Ren *et al.* [76] employed a novel technique for solving the stability issues of $CsPbX_3$ perovskite QDs by implanting $CsPbX_3$ perovskite QDs into mesoporous MOF-5 crystals (Figure 13d). It has been observed that the $CsPbX_3$/MOF composites have enhanced stability while keeping their excellent optical characteristics intact. The experimental findings revealed that, under 200 mA, $CsPbX_3$/MOF-5 W-LED produced hot white light and the PL maximum was in agreement with the PL bands of the corresponding $CsPbX_3$/MOF-5 (Figure 13e). From the CRI value (83) and luminous efficiency (21.6 lm W^{-1}), it has demonstrated the excellent efficacy of $CsPbX_3$/MOF-5 W-LED whereas the CIE color coordinate triangle of the $CsPbX_3$/MOF5 W-LED comprehends 124% of the National Television System Committee standard (Figure 13f).

3.6 Other applications

In addition to the aforementioned uses, QDs@MOFs have shown high potential for other promising applications thanks to their exceptional characteristics. Biodegradable drug delivery transporters with long-term drug release properties are useful in cancer therapy because they help to reduce some of the adverse effects. In this context, Pooresmaeil *et al.* [170] developed a simple technique for fabricating MOFs inside a carboxymethylcellulose (CMC)/GQD matrix, which is utilized for anticancer drugs. The findings revealed that the MIL-53@CMC/GQDs may be offered as a viable drug delivery vehicle. Furthermore, it was observed that MIL-53@CMC/GQDs have greater DOX-loading capacity than MIL-53, as demonstrated by the

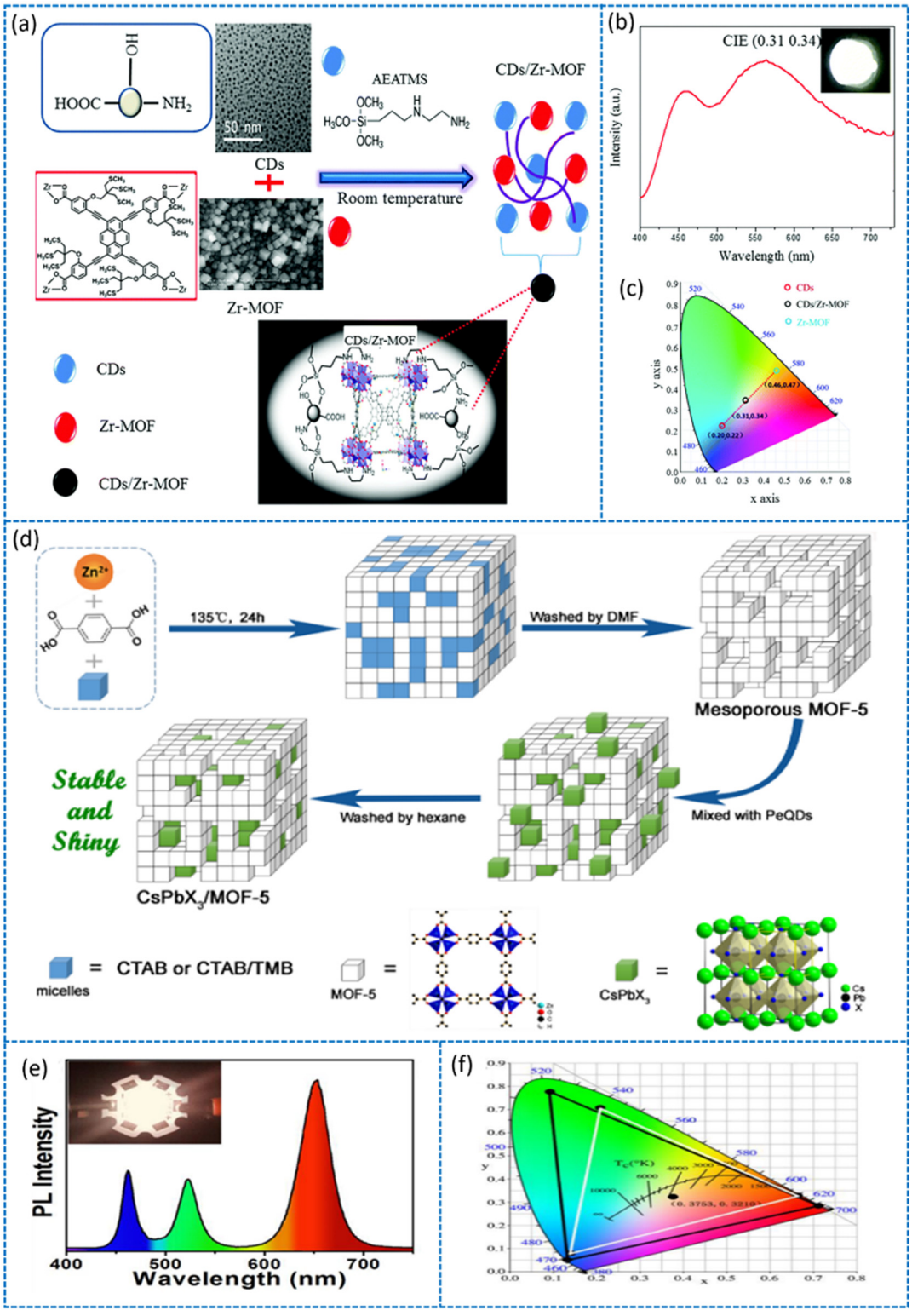

Figure 13: (a) Schematic representation of the construction of CDs/Zr-MOF. (b) Down-conversion WLED emission spectrum based on CDs/Zr-MOF coated on a 365 nm InGaN LED chip. (c) CIE chromaticity coordinates of (0.20, 0.22), (0.46, 0.47), and (0.31, 0.34) for the CDs LEDs, Zr-MOFs LEDs, and CDs/Zr-MOF WLEDs, respectively [123]. (d) Synthesis scheme of $CsPbX_3$/MOF-5 composites. (e) PL spectrum of $CsPbX_3$/MOF-5 WLED. (f) The CIE color coordinate triangle of $CsPbBr_3$/MOF-5 (green), CsPbBr0.6I2.4/MOF-5 (red), and InGaN (blue) correlated with the National Television System Committee standard (white line) [76].

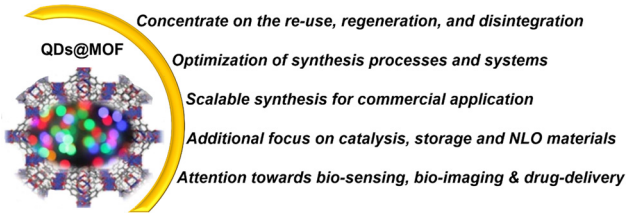

Figure 14: QDs@MOF: challenges and opportunities.

pH-dependent DOX release behavior in drug release tests, showing meticulous release actions *in vitro*, which is in good agreement with the first-order kinetic model and the non-Fickian mechanism. The cytocompatibility of MIL-53@CMC/GQDs against the human cancerous cell lines was confirmed using a cytotoxic test (MDA-MB 231). Furthermore, by following a step-by-step bisacrificial template scheme, Zhu *et al.* [220] were the first to report a bimetallic sulfide QDs, Cu_2SnS_3 (CTS)-involved MOF nanosheets, CuBDC (BDC = 1,4-benzenedicarboxylate). According to a Z-scan investigation conducted under the illumination of a 532 nm laser, the CTS@CuBDC film exhibited significant optical limiting (OL) performance and precise truncated OL thresholds ($0.92\,J\,cm^2$), along with high third-order nonlinear susceptibility (1.9×10^{-6} esu). This research shows that the new methodical approach (bisacrificial templates) to producing metal sulfide QD-distributed MOF hybrid composites is interesting and practical and might be a good option for nonlinear optical applications.

4 Conclusions and prospects

In this article, we have presented a comprehensive overview of advancements in QDs@MOF hybrids, covering synthetic techniques, structures, and applications. The produced QDs@MOF hybrid demonstrated improved stability as well as novel characteristics and application potential. Recently, QDs@MOFs have gained popularity because of their remarkable physicochemical and optical–electrical characteristics and are therefore considered a cutting-edge branch of materials. Various methodologies have been adopted by which QDs@MOFs endowed with a diversity of exclusive properties, such as exceptional PL characteristics, high selectivity to target analytes, or biocompatibility, can now be prepared. Furthermore, QDs@MOFs may be employed in a broader range of applications, including catalysis, sensing, bioimaging, optoelectronics, and batteries. Despite these amazing results, a number of obstacles illustrated in Figure 14 must be addressed to encourage further progress in this field.

1) The most straightforward way to adjust the characteristics of QDs@MOFs to specific applications is using the appropriate synthesis process. Many investigations have revealed that QDs@MOFs can be synthesized *via* a variety of methods. The ship–bottle/bottle–ship techniques are the most frequent in QDs@MOF synthesis, whereas photochemical decomposition/direct surface functionalization has received less attention. As a result, it is worthwhile to put more effort into QDs@MOF synthesis.
2) Controlling the morphology and surface properties of QDs@MOFs remains a daunting task. As a result, various experimental parameters, such as temperature, reaction duration, solvent impact, and reaction device, should be used more thoroughly to identify the growth mode. This can result in an MOF-based hybrid QD material with better morphologies and surface functionalization.
3) This field is still in its infancy and may not be appropriate for industrial manufacturing on a large scale. As a result, novel synthetic methodologies must be developed that will be not only cost-effective in terms of laboratory research but also suitable for massive commercial applications.
4) Many studies have shown that QDs@MOFs exhibit outstanding fluorescence behavior, photonic, photothermal transformation, and photoelectronic characteristics in tests. Even though these features of QDs@MOFs have been already demonstrated, there are still challenges to address. Right away, attention should be focused more on improving their current qualities and expanding these properties to other study domains. In this context, the combination of theoretical models and actual experiments will lead to successfully investigating novel QDs@MOFs with new and better properties.
5) Based on the categories of QDs@MOFs, it has been observed that most works were conducted employing CdS, CdSe, CdTe, GQDs, *etc.*, meaning that other QD materials should be paid greater attention to. MXene QDs, for example, have attractive features and have shown to be useful in energy production, catalysis, and sensing owing to extremely sensitive surface terminations. As a result, MXene QDs@MOF advancement is extremely desirable.
6) The majority of MOF hybrid QD materials addressed thus far were made of MOFs and single-QD materials. As a result, numerous different materials or MOFs

coupled with some other MOFs deserve further investigation.

7) Although a great deal of research has been done on QDs@MOF materials due to their versatile nature, their application is still a long way off. Solar cells, for example, are an important part of the solution to the worldwide energy crisis. Up to date, many resources have been investigated in the field of solar cells; nonetheless, certain drawbacks, such as short service life, low energy efficiency, or higher cost, have severely hampered their practical applicability. In the meantime, numerous studies have shown that QD-based materials are promising prospects for solar cell applications. Therefore, it is worth putting extra effort into investigating the use of QDs@MOFs in solar cells.
8) Furthermore, diverse hybridized QDs@MOFs enable a wide range of electrochemical applications, whereas studies related to NRR are rarely conducted.
9) Importantly, more research into the applicability of QDs@MOF-based immunosensing is required. Since there has been some research on bio(sensing)-based QDs@MOFs, more methodologies and unique protocols for the identification of cell cultures and cancer biomarkers should be developed.
10) The relevance of hybrid materials for applications requiring NLO characteristics, upconversion, and lasing has already been emphasized by the available results. Nevertheless, this is still a relatively new and developing field of study, and factors impacting, *e.g.*, the higher-order nonlinear optical features of QDs@MOF materials should be analyzed in an unswerving manner.
11) Currently, the preparation of perovskite-based MOF hybrid materials is a hot topic due to their various intriguing applications [223,224], but the eco-toxicity of heavy metal ions is a key problem for lead perovskites. As a result, additional effort must be invested in the future in investigating and developing novel nontoxic and environmentally acceptable materials for the perovskite@MOF composite.

In general, we have presented some of the most recent research findings of QDs@MOF. This study aims to provide in-depth knowledge about the variety of synthesis, characteristics, and uses of QDs@MOF, alongside stimulating future research into these new and fascinating domains. Despite the significant accomplishments, there are still some basic and technological gaps and obstacles in this area and, therefore, considerable effort should be put into the exploration of novel preparation techniques, physicochemical characteristics, and prospective applications. The abovementioned concerns must be addressed to stimulate continued progress in the synthesis and implementation of new QDs@MOF hybrids, which will have a substantial influence on chemistry, material science, and a broad range of applications.

Acknowledgments: The authors acknowledge ICT-IOC, Bhubaneswar, for providing necessary support. Rambabu Dandela thanks DST-SERB for the Ramanujan fellowship (SB/S2/RJN-075/2016), Core research grant (CRG/2018/000782), and ICT-IOC startup grant. MO gratefully acknowledges the support of the Ministry of Education, Youth and Sports of the Czech Republic and the Operational Programme for Research, Development and Education of the European Regional Development Fund (Project No. CZ.02.1.01/0.0/0.0/16_019/0000754) K. J. R. acknowledges support from the Indian Institute of Technology Jammu for providing a seed grant (SGT-100038) and SERB SRG/2020/000865.

Funding information: DST-SERB for the Ramanujan fellowship (SB/S2/RJN-075/2016), Core research grant (CRG/2018/000782), and ICT-IOC startup grant. Ministry of Education, Youth and Sports of the Czech Republic and the Operational Programme for Research, Development and Education of the European Regional Development Fund (Project No. CZ.02.1.01/0.0/0.0/16_019/0000754) K. J. R. acknowledges support from the Indian Institute of Technology Jammu for providing a seed grant (SGT-100038) and SERB SRG/2020/000865.

Author contributions: All authors have accepted responsibility for the entire content of this manuscript and approved its submission.

Conflict of interest: The authors state no conflict of interest.

References

[1] Yaghi OM, Li G, Li H. Selective binding and removal of guests in a microporous metal-organic framework. Nature. 1995;378:703–6.
[2] Yaghi OM, Li H. Hydrothermal synthesis of a metal-organic framework containing large rectangular channels. J Am Chem Soc. 1995;117:10401–2.
[3] Lee J, Farha OK, Roberts J, Scheidt KA, Nguyen ST, Hupp JT. Metal-organic framework materials as catalysts. Chem Soc Rev. 2009;38:1450–9.
[4] Herm ZR, Wiers BM, Mason JA, van Baten JM, Hudson MR, Zajdel P, et al. Separation of hexane isomers in a metal-organic framework with triangular channels. Science (80-). 2013;340:960–4.

[5] Qiu S, Xue M, Zhu G. Metal-organic framework membranes: from synthesis to separation application. Chem Soc Rev. 2014;43:6116–40.
[6] Farrusseng D, Aguado S, Pinel C. Metal-organic frameworks: opportunities for catalysis. Angew Chemie Int Ed. 2009;48:7502–13.
[7] Yang P, Liu Q, Liu J, Zhang H, Li Z, Li R, et al. Interfacial growth of a metal-organic framework (UiO-66) on functionalized graphene oxide (GO) as a suitable seawater adsorbent for extraction of uranium(VI). J Mater Chem A. 2017;5:17933–42.
[8] Liu H, Liu B, Lin LC, Chen G, Wu Y, Wang J, et al. A hybrid absorption-adsorption method to efficiently capture carbon. Nat Commun. 2014;5:5147. doi: 10.1038/ncomms6147. Epub ahead of print.
[9] Kang Z, Fan L, Sun D. Recent advances and challenges of metal-organic framework membranes for gas separation. J Mater Chem A. 2017;5:10073–91.
[10] Hendon CH, Rieth AJ, Korzyński MD, Dincă M. Grand challenges and future opportunities for metal-organic frameworks. ACS Cent Sci. 2017;3:554–63.
[11] Rosseinsky MJ. Perspective: metal-organic frameworks – opportunities and challenges. APL Mater. 2014;2:124001.
[12] Freund R, Zaremba O, Arnauts G, Ameloot R, Skorupskii G, Dincă M, et al. The current status of MOF and COF applications. Angew Chemie Int Ed. 2021;60:23975–4001.
[13] Yang C, Shang S, Gu Q, Shang J, Li X. Metal-organic framework-derived carbon nanotubes with multi-active Fe-N/Fe sites as a bifunctional electrocatalyst for zinc-air battery. J Energy Chem. 2022;66:306–13.
[14] Xu Y, Liu M, Wang M, Ren T, Ren K, Wang Z, et al. Methanol electroreforming coupled to green hydrogen production over bifunctional NiIr-based metal-organic framework nanosheet arrays. Appl Catal B Environ. 2022;300:120753. doi: 10.1016/j.apcatb.2021.120753. Epub ahead of print.
[15] Yadav P, Chatterjee K, Saini DK. Two-dimensional MOF-based liquid marbles: surface energy calculations and efficient oil-water separation using a ZIF-9-III@PVDF membrane. J Mater Chem A. 2021;9:23651–9.
[16] Liu X, Guan C, Hu Y, Zhang L, Elshahawy AM, Wang J. 2D Metal-organic frameworks derived nanocarbon arrays for substrate enhancement in flexible supercapacitors. Small. 2018;14:1702641. doi: 10.1002/smll.201702641. Epub ahead of print.
[17] Zhao C, Dai X, Yao T, Chen W, Wang X, Wang J, et al. Ionic exchange of metal organic frameworks to access single nickel sites for efficient electroreduction of CO_2. J Am Chem Soc. 2017;139:8078–81.
[18] Yaghi OM, O'keeffe M, Ockwig NW, Chae HK, Eddaoudi M, Kim J. Reticular synthesis and the design of new materials. Nature. 2003;423:705–14.
[19] Tian H-R, Zhang Z, Liu S-M, Dang TY, Li XH, Lu Y, et al. A novel polyoxovanadate-based Co-MOF: highly efficient and selective oxidation of a mustard gas simulant by two-site synergetic catalysis. J Mater Chem A. 2020;8:12398–405.
[20] Alqadami AA, Naushad M, Alothman ZA, Ghfar AA. Novel metal-organic framework (MOF) based composite material for the sequestration of U(VI) and Th(IV) metal ions from aqueous environment. ACS Appl Mater Interfaces. 2017;9:36026–37.
[21] Huang X, Yan S, Deng D, Zhang L, Liu R, Lv Y. Novel strategy for engineering the metal-oxide@MOF core@shell architecture and its applications in cataluminescence sensing. ACS Appl Mater Interfaces. 2021;13:3471–80.
[22] Zhang M, Dai Q, Zheng H, Chen M, Dai L. Novel MOF-derived Co@N-C bifunctional catalysts for highly efficient Zn-air batteries and water splitting. Adv Mater. 2018;30:1705431.
[23] Wang K, Tao X, Xu J, Yin N. Novel chitosan-MOF composite adsorbent for the removal of heavy metal ions. Chem Lett. 2016;45:1365–8.
[24] Soltani R, Pelalak R, Pishnamazi M, Marjani A, Albadarin AB, Sarkar SM, et al. A novel and facile green synthesis method to prepare LDH/MOF nanocomposite for removal of Cd(II) and Pb(II). Sci Rep. 2021;11:1609.
[25] Farhadi S, Riahi-Madvar A, Sargazi G, Mortazavi M. Immobilization of lepidium draba peroxidase on a novel Zn-MOF nanostructure. Int J Biol Macromol. 2021;173:366–78.
[26] Dang S, Zhu Q-L, Xu Q. Nanomaterials derived from metal-organic frameworks. Nat Rev Mater. 2017;3:17075.
[27] Saad A, Biswas S, Gkaniatsou E, Sicard C, Dumas E, Menguy N, et al. Metal-organic framework based 1D nanostructures and their superstructures: synthesis, microstructure, and properties. Chem Mater. 2021;33:5825–49.
[28] Wu C, Liu Q, Chen R, Liu J, Zhang H, Li R, et al. Fabrication of ZIF-8@SiO_2 micro/nano hierarchical superhydrophobic surface on AZ31 magnesium alloy with impressive corrosion resistance and abrasion resistance. ACS Appl Mater Interfaces. 2017;9:11106–15.
[29] Liu C, Lin L, Sun Q, Wang J, Huang R, Chen W, et al. Site-specific growth of MOF-on-MOF heterostructures with controllable nano-architectures: beyond the combination of MOF analogues. Chem Sci. 2020;11:3680–6.
[30] Xia W, Mahmood A, Zou R, Xu Q. Metal-organic frameworks and their derived nanostructures for electrochemical energy storage and conversion. Energy Environ Sci. 2015;8:1837–66.
[31] Yan R, Ma T, Cheng M, Tao X, Yang Z, Ran F, et al. Metal-organic-framework-derived nanostructures as multifaceted electrodes in metal-sulfur batteries. Adv Mater. 2021;33:2008784.
[32] Rashti A, Lu X, Dobson A, Hassani E, Feyzbar-Khalkhali-Nejad F, He K, et al. Tuning MOF-derived Co_3O_4/$NiCo_2O_4$ nanostructures for high-performance energy storage. ACS Appl Energy Mater. 2021;4:1537–47.
[33] Mei C, Hou S, Liu M, Guo Y, Liu T, Li J, et al. MOF derived $ZnFe_2O_4$ nanoparticles scattered in hollow octahedra carbon skeleton for advanced lithium-ion batteries. Appl Surf Sci. 2021;541:148475.
[34] Jagadeesh RV, Murugesan K, Alshammari AS, Neumann H, Pohl MM, Radnik J, et al. MOF-derived cobalt nanoparticles catalyze a general synthesis of amines. Science (80–). 2017;358:326–32.
[35] Fan H, Peng M, Strauss I, Mundstock A, Meng H, Caro J. MOF-in-COF molecular sieving membrane for selective hydrogen separation. Nat Commun. 2021;12:38.
[36] Fu L, Yang Z, Wang Y, Li R, Zhai J. Construction of metal-organic frameworks (MOFs)-based membranes and their ion transport applications. Small Sci. 2021;1:2000035.
[37] Li X, Liu Y, Wang J, Gascon J, Li J, Van der Bruggen B. Metal-organic frameworks based membranes for liquid separation. Chem Soc Rev. 2017;46:7124–44.
[38] Zhu J, Qin L, Uliana A, Hou J, Wang J, Zhang Y, et al. Elevated performance of thin film nanocomposite membranes enabled by modified hydrophilic MOFs for nanofiltration. ACS Appl Mater Interfaces. 2017;9:1975–86.

[39] Zhu J, Hou J, Yuan S, Zhao Y, Li Y, Zhang R, et al. MOF-positioned polyamide membranes with a fishnet-like structure for elevated nanofiltration performance. J Mater Chem A. 2019;7:16313–22.
[40] Chen L-J, Zhao X, Liu Y-Y, Yan XP. Macrophage membrane coated persistent luminescence nanoparticle@MOF-derived mesoporous carbon core-shell nanocomposites for autofluorescence-free imaging-guided chemotherapy. J Mater Chem B. 2020;8:8071–83.
[41] Katayama Y, Bentz KC, Cohen SM. Defect-free MOF-based mixed-matrix membranes obtained by corona cross-linking. ACS Appl Mater Interfaces. 2019;11:13029–37.
[42] Fu J, Das S, Xing G, Ben T, Valtchev V, Qiu S. Fabrication of COF-MOF composite membranes and their highly selective separation of H_2/CO_2. J Am Chem Soc. 2016;138:7673–80.
[43] Li W, Zhang Y, Zhang C, Meng Q, Xu Z, Su P, et al. Transformation of metal-organic frameworks for molecular sieving membranes. Nat Commun. 2016;7:11315.
[44] Ji Y-L, Gu B-X, Xie S-J, Yin MJ, Qian WJ, Zhao Q, et al. Superfast water transport zwitterionic polymeric nanofluidic membrane reinforced by metal-organic frameworks. Adv Mater. 2021;33:2102292.
[45] Wei Y-S, Zhang M, Kitta M, Liu Z, Horike S, Xu Q. A single-crystal open-capsule metal-organic framework. J Am Chem Soc. 2019;141:7906–16.
[46] Ameloot R, Vermoortele F, Vanhove W, Roeffaers MB, Sels BF, De Vos DE. Interfacial synthesis of hollow metal-organic framework capsules demonstrating selective permeability. Nat Chem. 2011;3:382–7.
[47] Carné-Sánchez A, Imaz I, Cano-Sarabia M, Maspoch D. A spray-drying strategy for synthesis of nanoscale metal-organic frameworks and their assembly into hollow superstructures. Nat Chem. 2013;5:203–11.
[48] Li W, Zhang Y, Xu Z, Meng Q, Fan Z, Ye S, et al. Assembly of MOF microcapsules with size-selective permeability on cell walls. Angew Chem Int Ed. 2016;55:955–9.
[49] Xu Z, Xiao G, Li H, Shen Y, Zhang J, Pan T, et al. Compartmentalization within self-assembled metal-organic framework nanoparticles for tandem reactions. Adv Funct Mater. 2018;28:1802479. doi: 10.1002/adfm.201802479. Epub ahead of print.
[50] Huo J, Marcello M, Garai A, Bradshaw D. MOF-polymer composite microcapsules derived from pickering emulsions. Adv Mater. 2013;25:2717–22.
[51] Ishiwata T, Michibata A, Kokado K, Ferlay S, Hosseini MW, Sada K. Box-like gel capsules from heterostructures based on a core-shell MOF as a template of crystal crosslinking. Chem Commun. 2018;54:1437–40.
[52] Yang H, Bradley SJ, Chan A, Waterhouse GI, Nann T, Kruger PE, et al. Catalytically active bimetallic nanoparticles supported on porous carbon capsules derived from metal-organic framework composites. J Am Chem Soc. 2016;138:11872–81.
[53] Cai G, Ding M, Wu Q, Jiang HL. Encapsulating soluble active species into hollow crystalline porous capsules beyond integration of homogeneous and heterogeneous catalysis. Natl Sci Rev. 2020;7:37–45.
[54] Tajik S, Orooji Y, Karimi F, Ghazanfari Z, Beitollahi H, Shokouhimehr M, et al. High performance of screen-printed graphite electrode modified with Ni-Mo-MOF for voltammetric determination of amaranth. J Food Meas Charact. 2021;15:4617–22.
[55] Rabiee N, Bagherzadeh M, Jouyandeh M, Zarrintaj P, Saeb MR, Mozafari M, et al. Natural polymers decorated mof-mxene nanocarriers for co-delivery of doxorubicin/pCRISPR. ACS Appl Bio Mater. 2021;4:5106–21.
[56] Rani S, Sharma B, Malhotra R, Kumar S, Varma RS, Dilbaghi N. Sn-MOF@CNT nanocomposite: an efficient electrochemical sensor for detection of hydrogen peroxide. Environ Res. 2020;191:110005.
[57] Bao Y, Chen Y, Lim T-T, Wang R, Hu X. A novel metal-organic framework (MOF)-mediated interfacial polymerization for direct deposition of polyamide layer on ceramic substrates for nanofiltration. Adv Mater Interfaces. 2019;6:1900132.
[58] Schmidt BVKJ. Metal-organic frameworks in polymer science: polymerization catalysis, polymerization environment, and hybrid materials. Macromol Rapid Commun. 2020;41:1900333.
[59] Ye B, Jiang R, Yu Z, Hou Y, Huang J, Zhang B, et al. Pt (111) quantum dot engineered Fe-MOF nanosheet arrays with porous core-shell as an electrocatalyst for efficient overall water splitting. J Catal. 2019;380:307–17.
[60] Zhao Y. A new era of metal-organic framework nanomaterials and applications. ACS Appl Nano Mater. 2020;3:4917–9.
[61] Sharma K, Raizada P, Hasija V, Singh P, Bajpai A, Nguyen VH, et al. ZnS-based quantum dots as photocatalysts for water purification. J Water Process Eng. 2021;43:102217.
[62] Jouyandeh M, Mousavi Khadem SS, Habibzadeh S, Esmaeili A, Abida O, Vatanpour V, et al. Quantum dots for photocatalysis: synthesis and environmental applications. Green Chem. 2021;23:4931–54.
[63] Iravani S, Varma RS. Green synthesis, biomedical and biotechnological applications of carbon and graphene quantum dots. A review. Environ Chem Lett. 2020;18:703–27.
[64] Yoo D, Park Y, Cheon B, Park MH. Carbon dots as an effective fluorescent sensing platform for metal ion detection. Nanoscale Res Lett. 2019;14:272.
[65] Jiang Y, Weiss EA. Colloidal quantum dots as photocatalysts for triplet excited state reactions of organic molecules. J Am Chem Soc. 2020;142:15219–29.
[66] Moon BJ, Kim SJ, Lee A, Oh Y, Lee SK, Lee SH, et al. Structure-controllable growth of nitrogenated graphene quantum dots via solvent catalysis for selective C–N bond activation. Nat Commun. 2021;12:5879.
[67] Kang S, Kim KM, jung K, Son Y, Mhin S, Ryu JH, et al. Graphene oxide quantum dots derived from coal for bioimaging: facile and green approach. Sci Rep. 2019;9:4101.
[68] Shaik SA, Sengupta S, Varma RS, Gawande MB, Goswami A. Syntheses of N-doped carbon quantum dots (NCQDs) from bioderived precursors: a timely update. ACS Sustain Chem Eng. 2021;9:3–49.
[69] Kwon J, Jun SW, Choi SI, Mao X, Kim J, Koh EK, et al. FeSe quantum dots for in vivo multiphoton biomedical imaging. Sci Adv. 2021;5:eaay0044.
[70] Fujii M, Fujii R, Takada M, Sugimoto H. Silicon quantum dot supraparticles for fluorescence bioimaging. ACS Appl Nano Mater. 2020;3:6099–107.
[71] Sun Y, Zheng S, Liu L, Kong Y, Zhang A, Xu K, et al. The cost-effective preparation of green fluorescent carbon dots for

bioimaging and enhanced intracellular drug delivery. Nanoscale Res Lett. 2020;15:55.
[72] Zhang W, Ding S, Zhuang W, Wu D, Liu P, Qu X, et al. InP/ZnS/ZnS core/shell blue quantum dots for efficient light-emitting diodes. Adv Funct Mater. 2020;30:2005303. doi: 10.1002/adfm.202005303. Epub ahead of print.
[73] Arif O, Zannier V, Rossi F, Ercolani D, Beltram F, Sorba L. Self-catalyzed InSb/InAs quantum dot nanowires. Nanomaterials. 2021;11:179. doi: 10.3390/nano11010179. Epub ahead of print.
[74] Wan S, Ou M, Zhong Q, Wang X. Perovskite-type CsPbBr3 quantum dots/UiO-66(NH2) nanojunction as efficient visible-light-driven photocatalyst for CO2 reduction. Chem Eng J. 2019;358:1287–95.
[75] Qiao GY, Guan D, Yuan S, Rao H, Chen X, Wang JA, et al. Perovskite quantum dots encapsulated in a mesoporous metal-organic framework as synergistic photocathode materials. J Am Chem Soc. 2021;143:14253–60.
[76] Ren J, Li T, Zhou X, Dong X, Shorokhov AV, Semenov MB, et al. Encapsulating all-inorganic perovskite quantum dots into mesoporous metal organic frameworks with significantly enhanced stability for optoelectronic applications. Chem Eng J. 2019;358:30–9.
[77] Wang YY, Ji XY, Yu M, Tao J. Confining lead-free perovskite quantum dots in metal-organic frameworks for visible light-driven proton reduction. Mater Chem Front. 2021;5:7796–807.
[78] Wageh S, Al-Ghamdi AA, Al-Zahrani AA, Driss H. High quantum yield Cu doped CdSe quantum dots. Mater Res Exp. 2019;6:0850d4. doi: 10.1088/2053-1591/ab268f. Epub ahead of print.
[79] Xie Y, Zheng J, Wang Y, Wang J, Yang Y, Liu X, et al. One-step hydrothermal synthesis of fluorescence carbon quantum dots with high product yield and quantum yield. Nanotechnology. 2019;30:085406. doi: 10.1088/1361-6528/aaf3fb. Epub ahead of print.
[80] Zheng J, Xie Y, Wei Y, Yang Y, Liu X, Chen Y, et al. An efficient synthesis and photoelectric properties of green carbon quantum dots with high fluorescent quantum yield. Nanomaterials. 2020;10:82. doi: 10.3390/nano10010082. Epub ahead of print.
[81] Wei Y, Chen L, Zhao S, Liu X, Yang Y, Du J, et al. Green-emissive carbon quantum dots with high fluorescence quantum yield: preparation and cell imaging. Front Mater Sci. 2021;15:253–65.
[82] Vallés-Pelarda M, Gualdrón-Reyes AF, Felip-León C, Angulo-Pachón CA, Agouram S, Muñoz-Sanjosé V, et al. High optical performance of cyan-emissive CsPbBr3 perovskite quantum dots embedded in molecular organogels. Adv Opt Mater. 2021;9:2001786. doi: 10.1002/adom.202001786. Epub ahead of print.
[83] Lohani J, Yadav S, Tyagi R, Sapra S. Efficient fluorescence quenching of CdSe quantum dots on epitaxial GaAs nanostructures. J Nanoparticle Res. 2019;21:205. doi: 10.1007/s11051-019-4649-4. Epub ahead of print.
[84] Liang Z, Kang M, Payne GF, Wang X, Sun R. Probing Energy and electron transfer mechanisms in fluorescence quenching of biomass carbon quantum dots. ACS Appl Mater Interfaces. 2016;8:17478–88.
[85] Yang L, Wen J, Li K, Liu L, Wang W. Carbon quantum dots: Comprehensively understanding of the internal quenching mechanism and application for catechol detection. Sens Actuators B Chem. 2021;333:129557. doi: 10.1016/j.snb.2021.129557. Epub ahead of print.
[86] Bag PP, Wang X-S, Sahoo P, Xiong J, Cao R. Efficient photocatalytic hydrogen evolution under visible light by ternary composite CdS@NU-1000/RGO. Catal Sci Technol. 2017;7:5113–9.
[87] Zhao H, Yu X, Li CF, Yu W, Wang A, Hu ZY, et al. Carbon quantum dots modified TiO2 composites for hydrogen production and selective glucose photoreforming. J Energy Chem. 2022;64:201–8.
[88] Zhao C, Zhou Y, Shi T, Guo D, Yin H, Song C, et al. Employing synergetic effect of ZnSe quantum dots and layered Ni(OH)(2) to boost the performance of lithium-sulfur cathodes. Nanotechnology. 2021;32:50. doi: 10.1088/1361-6528/ac2982. Epub ahead of print.
[89] Nagaraj G, Mohammed MKA, Shekargoftar M, Sasikumar P, Sakthivel P, Ravi G, et al. High-performance perovskite solar cells using the graphene quantum dot-modified SnO2/ZnO photoelectrode. Mater Today Energy. 2021;22:100853. doi: 10.1016/j.mtener.2021.100853. Epub ahead of print.
[90] Cao B, Liu H, Zhang X, Zhang P, Zhu Q, Du H, et al. MOF-derived ZnS nanodots/$Ti_3C_2T_x$ MXene hybrids boosting superior lithium storage performance. Nano-Micro Lett. 2021;13:202. doi: 10.1007/s40820-021-00728-x. Epub ahead of print.
[91] Abdelbar MF, Abdelhameed M, Esmat M, El-Kemary M, Fukata N. Energy management in hybrid organic-silicon nanostructured solar cells by downshifting using CdZnS/ZnS and CdZnSe/ZnS quantum dots. Nano Energy. 2021;89:106470. doi: 10.1016/j.nanoen.2021.106470. Epub ahead of print.
[92] Swarnkar A, Marshall AR, Sanehira EM, Chernomordik BD, Moore DT, Christians JA, et al. Quantum dot-induced phase stabilization of alpha-CsPbI3 perovskite for high-efficiency photovoltaics. Science (80–). 2016;354:92–5.
[93] Chiba T, Hayashi Y, Ebe H, Hoshi K, Sato J, Sato S, et al. Anion-exchange red perovskite quantum dots with ammonium iodine salts for highly efficient light-emitting devices. Nat Photonics. 2018;12:681–7.
[94] Sun C, Zhang Y, Ruan C, Yin C, Wang X, Wang Y, et al. Efficient and stable white LEDs with silica-coated inorganic perovskite quantum dots. Adv Mater. 2016;28:10088–94.
[95] Yee PY, Brittman S, Mahadik NA, Tischler JG, Stroud RM, Efros AL, et al. Cu2-xS/PbS core/shell nanocrystals with improved chemical stability. Chem Mater. 2021;33:6685–91.
[96] Rani S, Sharma B, Kapoor S, Malhotra R, Varma RS, Dilbaghi N. Construction of silver quantum dot immobilized Zn-MOF-8 composite for electrochemical sensing of 2,4-dinitrotoluene. Appl Sci. 2019;9:4952. doi: 10.3390/app9224952. Epub ahead of print.
[97] Yu H, Jing Y, Du CF, Wang J. Tuning the reversible chemisorption of hydroxyl ions to promote the electrocatalysis on ultrathin metal-organic framework nanosheets. J Energy Chem. 2022;65:71–7.
[98] Qian Y, Zhang F, Pang H. A review of MOFs and their composites-based photocatalysts: synthesis and applications. Adv Funct Mater. 2021;31:2104231.
[99] Wang Y, Wang M, Wang X, Ma W, Liu J, Li J. Designed synthesis of CD@Cu-ZIF-8 composites as excellent peroxidase

mimics for assaying glutathione. Mater Chem Front. 2021;5:6125–32.
[100] Kar MR, Ray S, Patra BK, Bhaumik S. State of the art and prospects of metal halide perovskite core@shell nanocrystals and nanocomposites. Mater Today Chem. 2021;20:100424. doi: 10.1016/j.mtchem.2021.100424. Epub ahead of print.
[101] Zhao Y, Xie C, Zhang X, Yang P. CsPbX3 quantum dots embedded in zeolitic imidazolate framework-8 microparticles for bright white light-emitting devices. ACS Appl Nano Mater. 2021;4:5478–85.
[102] Zareba JK, Nyk M, Samoc M. Nonlinear optical properties of emerging nano- and microcrystalline materials. Adv Opt Mater. 2021;9:2100216. doi: 10.1002/adom.202100216.
[103] Kumagai K, Uematsu T, Torimoto T, Kuwabata S. Variations in Photoluminescence intensity of a quantum dot assembly investigated by its adsorption on cubic metal-organic frameworks. J Phys Chem C. 2021;125:8285–93.
[104] Saroha R, Oh JH, Seon YH, Kang YC, Lee JS, Jeong DW, et al. Freestanding interlayers for Li–S batteries: design and synthesis of hierarchically porous N-doped C nanofibers comprising vanadium nitride quantum dots and MOF-derived hollow N-doped C nanocages. J Mater Chem A. 2021;9:11651–64.
[105] Safa S, Khajeh M, Oveisi AR, Azimirad R, Salehzadeh H. Photocatalytic performance of graphene quantum dot incorporated UiO-66-NH2 composite assembled on plasma-treated membrane. Adv Powder Technol. 2021;32:1081–7.
[106] Chen M, Liu T, Zhang X, Zhang R, Tang S, Yuan Y, et al. Photoinduced enhancement of uranium extraction from seawater by MOF/black phosphorus quantum dots heterojunction anchored on cellulose nanofiber aerogel. Adv Funct Mater. 2021;31:2100106.
[107] Gao S, Cen W, Li Q, Li J, Lu Y, Wang H, et al. A mild one-step method for enhancing optical absorption of amine-functionalized metal-organic frameworks. Appl Catal B Environ. 2018;227:190–7.
[108] Gao Y, Wu J, Zhang W, Tan Y, Zhao J, Tang B. The electrochemical performance of SnO_2 quantum dots@zeolitic imidazolate frameworks-8 (ZIF-8) composite material for supercapacitors. Mater Lett. 2014;128:208–11.
[109] Zhang D, Zhao J, Liu Q, Xia Z. Synthesis and luminescence properties of CsPbX3@Uio-67 composites toward stable photoluminescence convertors. Inorg Chem. 2019;58:1690–6.
[110] Meng X, Zhang C, Zhuang J, Zheng G, Zhou L. Metal-organic framework as nanoreactors to co-incorporate carbon nanodots and CdS quantum dots into the pores for improved H_2 evolution without noble-metal cocatalyst. Appl Catal B Environ. 2019;244:340–6.
[111] Kaur R, Sharma AL, Kim K-H, Deep A. A novel CdTe/Eu-MOF photoanode for application in quantum dot-sensitized solar cell to improve power conversion efficiency. J Ind Eng Chem. 2017;53:77–81.
[112] Mo G, Qin D, Jiang X, Zheng X, Mo W, Deng B. A sensitive electrochemiluminescence biosensor based on metal-organic framework and imprinted polymer for squamous cell carcinoma antigen detection. Sens Actuators B Chem. 2020;310:127852.
[113] Wang K, Li N, Zhang J, Zhang Z. Size-selective QD@MOF core-shell nanocomposites for the highly sensitive monitoring of oxidase activities. Biosens Bioelectron. 2017;87:339–44.
[114] Wang H, Yuan X, Wu Y, Chen X, Leng L, Zeng G. Photodeposition of metal sulfides on titanium metal-organic frameworks for excellent visible-light-driven photocatalytic Cr(VI) reduction. RSC Adv. 2015;5:32531–5.
[115] Lin R, Shen L, Ren Z, Wu W, Tan Y, Fu H, et al. Enhanced photocatalytic hydrogen production activity via dual modification of MOF and reduced graphene oxide on CdS. Chem Commun. 2014;50:8533–5.
[116] Jin S, Son H-J, Farha OK, Wiederrecht GP, Hupp JT. Energy transfer from quantum dots to metal-organic frameworks for enhanced light harvesting. J Am Chem Soc. 2013;135:955–8.
[117] Mondal T, Haldar D, Ghosh A, Ghorai UK, Saha SK. A MOF functionalized with CdTe quantum dots as an efficient white light emitting phosphor material for applications in displays. New J Chem. 2020;44:55–63.
[118] Yang Q, Wang Q, Long Y, Wang F, Wu L, Pan J, et al. *In situ* formation of Co9S8 quantum dots in MOF-derived ternary metal layered double hydroxide nanoarrays for high-performance hybrid supercapacitors. Adv Energy Mater. 2020;10:1903193.
[119] Huang Z, Chen H, Zhao L, He X, Fang W, Du Y, et al. CdSe QDs sensitized MIL-125/TiO2@SiO2 biogenic hierarchical composites with enhanced photocatalytic properties via two-level heterostructure. J Mater Sci Mater Electron. July 2018;29:1-12054. doi: 10.1007/s10854-018-9310-y. Epub ahead of print.
[120] Jin M, Mou ZL, Zhang R-L, Liang SS, Zhang ZQ. An efficient ratiometric fluorescence sensor based on metal-organic frameworks and quantum dots for highly selective detection of 6-mercaptopurine. Biosens Bioelectron. 2017;91:162–8.
[121] Li Z, Bu F, Wei J, Yao W, Wang L, Chen Z, et al. Boosting the energy storage densities of supercapacitors by incorporating N-doped graphene quantum dots into cubic porous carbon. Nanoscale. 2018;10:22871–83.
[122] Li Z, Liu X, Wang L, Bu F, Wei J, Pan D, et al. Hierarchical 3D all-carbon composite structure modified with N-doped graphene quantum dots for high-performance flexible supercapacitors. Small. 2018;14:1801498.
[123] Wang A, Hou Y-L, Kang F, Lyu F, Xiong Y, Chen WC, et al. Rare earth-free composites of carbon dots/metal-organic frameworks as white light emitting phosphors. J Mater Chem C. 2019;7:2207–11.
[124] Wang Y, He J, Zheng M, Qin M, Wei W. Dual-emission of Eu based metal-organic frameworks hybrids with carbon dots for ratiometric fluorescent detection of Cr(VI). Talanta. 2019;191:519–25.
[125] Wang XZ, Zhang ZQ, Guo R, Zhang YY, Zhu NJ, Wang K, et al. Dual-emission CdTe quantum dot@ZIF-365 ratiometric fluorescent sensor and application for highly sensitive detection of l-histidine and Cu^{2+}. Talanta. 2020;217:121010.
[126] Xie S, Li X, Wang L, Zhu F, Zhao X, Yuan T, et al. High quantum-yield carbon dots embedded metal-organic frameworks for selective and sensitive detection of dopamine. Microchem J. 2021;160:105718.
[127] Zhou L, Shan X, Jiang D, Wang W, Chen Z. Electrochemical luminescence sensor based on CDs@HKUST-1 composite for detection of catechol. J Electroanal Chem. 2020;871:114215.

[128] Yang J-M, Hu X-W, Liu Y-X, Zhang W. Fabrication of a carbon quantum dots-immobilized zirconium-based metal-organic framework composite fluorescence sensor for highly sensitive detection of 4-nitrophenol. Microp Mesop Mater. 2019;274:149–54.
[129] He L, Wang T, An J, Li X, Zhang L, Li L, et al. Carbon nanodots@zeolitic imidazolate framework-8 nanoparticles for simultaneous pH-responsive drug delivery and fluorescence imaging. CrystEngComm. 2014;16:3259–63.
[130] Qin Y-T, Feng Y-S, Ma Y-J, He XW, Li WY, Zhang YK. Tumor-sensitive biodegradable nanoparticles of molecularly imprinted polymer-stabilized fluorescent zeolitic imidazolate framework-8 for targeted imaging and drug delivery. ACS Appl Mater Interfaces. 2020;12:24585–98.
[131] Liu J, Liu T, Du P, Zhang L, Lei J. Metal-organic framework (MOF) hybrid as a tandem catalyst for enhanced therapy against hypoxic tumor cells. Angew Chemie Int Ed. 2019;58:7808–12.
[132] Tian Z, Yao X, Ma K, Niu X, Grothe J, Xu Q, et al. Metal-organic framework/graphene quantum dot nanoparticles used for synergistic chemo- and photothermal therapy. ACS Omega. 2017;2:1249–58.
[133] Lin R, Li S, Wang J, Xu J, Xu C, Wang J, et al. Facile generation of carbon quantum dots in MIL-53(Fe) particles as localized electron acceptors for enhancing their photocatalytic Cr(VI) reduction. Inorg Chem Front. 2018;5:3170–7.
[134] Guo M, Chi J, Li Y, Waterhouse G, Ai S, Hou J, et al. Fluorometric determination of mercury(II) based on dual-emission metal-organic frameworks incorporating carbon dots and gold nanoclusters. Microchim Acta. 2020;187:534.
[135] Guo H, Wang X, Wu N, Xu M, Wang M, Zhang L, et al. In-situ synthesis of carbon dots-embedded europium metal-organic frameworks for ratiometric fluorescence detection of Hg^{2+} in aqueous environment. Anal Chim Acta. 2021;1141:13–20.
[136] Zhang Y, Zhou K, Qiu Y, Xia L, Xia Z, Zhang K, et al. Strongly emissive formamide-derived N-doped carbon dots embedded Eu(III)-based metal-organic frameworks as a ratiometric fluorescent probe for ultrasensitive and visual quantitative detection of Ag. Sens Actuators B Chem. 2021;339:129922. doi: 10.1016/j.snb.2021.129922. Epub ahead of print.
[137] Guo H, Wang X, Wu N, Xu M, Wang M, Zhang L, et al. One-pot synthesis of a carbon dots@zeolitic imidazolate framework-8 composite for enhanced Cu^{2+} sensing. Anal Methods. 2020;12:4058–63.
[138] Bera MK, Behera L, Mohapatra S. A fluorescence turn-down-up detection of Cu^{2+} and pesticide quinalphos using carbon quantum dot integrated UiO-66-NH_2. Colloids Surf A Physicochem Eng Asp. 2021;624:126792.
[139] Asadi F, Azizi SN, Chaichi MJ. Green synthesis of fluorescent PEG-ZnS QDs encapsulated into Co-MOFs as an effective sensor for ultrasensitive detection of copper ions in tap water. Mater Sci Eng C Mater Biol Appl. 2019;105:110058.
[140] Guo X, Pan Q, Song X, Guo Q, Zhou S, Qiu J, et al. Embedding carbon dots in Eu^{3+} -doped metal-organic framework for label-free ratiometric fluorescence detection of Fe^{3+} ions. J Am Ceram Soc. 2021;104:886–95.
[141] Xu H, Zhou S, Xiao L, Wang H, Li S, Yuan Q. Fabrication of a nitrogen-doped graphene quantum dot from MOF-derived porous carbon and its application for highly selective fluorescence detection of Fe^{3+}. J Mater Chem C. 2015;3:291–7.
[142] Fan L, Wang Y, Li L, Zhou J. Carbon quantum dots activated metal organic frameworks for selective detection of Cu(II) and Fe(III). Colloids Surf A Physicochem Eng Asp. 2020;588:124378. doi: 10.1016/j.colsurfa.2019.124378. Epub ahead of print.
[143] Zhang D, Xu Y, Liu Q, Xia Z. Encapsulation of $CH_3NH_3PbBr_3$ perovskite quantum dots in MOF-5 microcrystals as a stable platform for temperature and aqueous heavy metal ion detection. Inorg Chem. 2018;57:4613–9.
[144] Wu J-X, Yan B. A dual-emission probe to detect moisture and water in organic solvents based on green-Tb^{3+} post-coordinated metal-organic frameworks with red carbon dots. Dalt Trans. 2017;46:7098–105.
[145] Fan M, Gan T, Yin G, Cheng F, Zhao N. Molecularly imprinted polymer coated Mn-doped ZnS quantum dots embedded in a metal-organic framework as a probe for selective room temperature phosphorescence detection of chlorpyrifos. RSC Adv. 2021;11:27845–54.
[146] Devi S, Shaswat S, Kumar V, Sachdev A, Gopinath P, Tyagi S. Nitrogen-doped carbon quantum dots conjugated isoreticular metal-organic framework-3 particles based luminescent probe for selective sensing of trinitrotoluene explosive. Microchim Acta. 2020;187:536.
[147] Chen L, Liu D, Zheng L, Yi S, He H. A structure-dependent ratiometric fluorescence sensor based on metal-organic framework for detection of 2,6-pyridinedicarboxylic acid. Anal Bioanal Chem. 2021;413:4227–36.
[148] Alivand MS, Tehrani N, Askarieh M, Ghasemy E, Esrafili MD, Ahmadi R, et al. Defect engineering-induced porosity in graphene quantum dots embedded metal-organic frameworks for enhanced benzene and toluene adsorption. J Hazard Mater. 2021;416:125973. doi: 10.1016/j.jhazmat.2021.125973. Epub ahead of print.
[149] Pashazadeh S, Habibi B. Determination of isoniazid by a copper-based metal-organic frameworks/carbon nitride quantum dots modified pencil graphite electrode as a highly sensitive and selective sensor. J Electroanal Chem. 2020;876:114493.
[150] Hu L, Song C, Shi T, Cui Q, Yang L, Li X, et al. Dual-quenching electrochemiluminescence resonance energy transfer system from IRMOF-3 coreaction accelerator enriched nitrogen-doped GQDs to ZnO@Au for sensitive detection of procalcitonin. Sens Actuators B Chem. 2021;346:130495. doi: 10.1016/j.snb.2021.130495. Epub ahead of print.
[151] Shokri R, Amjadi M. A ratiometric fluorescence sensor for triticonazole based on the encapsulated boron-doped and phosphorous-doped carbon dots in the metal organic framework. Spectrochim Acta Part A Mol Biomol Spectrosc. 2021;246:118951. doi: 10.1016/j.saa.2020.118951. Epub ahead of print.
[152] Du D, Shu J, Guo M, Haghighatbin MA, Yang D, Bian Z, et al. Potential-resolved differential electrochemiluminescence immunosensor for cardiac troponin I based on MOF-5-wrapped CdS quantum dot nanoluminophores. Anal Chem. 2020;92:14113–21.
[153] Zhang G, Chen S, Yang Y, Liu Y, Lei L, Liu X, et al. Boron nitride quantum dots decorated MIL-100(Fe) for boosting the photo-generated charge separation in photocatalytic

refractory antibiotics removal. Environ Res. 2021;202:111661. doi: 10.1016/j.envres.2021.111661. Epub ahead of print.
[154] Mousavi A, Zare-Dorabei R, Mosavi SH. A novel hybrid fluorescence probe sensor based on metal-organic framework@carbon quantum dots for the highly selective detection of 6-mercaptopurine. Anal Methods. 2020;12:5397–406.
[155] Wang K, Li N, Zhang J, Zhang Z, Dang F. Size-selective QD@MOF core-shell nanocomposites for the highly sensitive monitoring of oxidase activities. Biosens Bioelectron. 2017;87:339–44.
[156] Feng S, Pei F, Wu Y, Lv J, Hao Q, Yang T, et al. A ratiometric fluorescent sensor based on g-CNQDs@Zn-MOF for the sensitive detection of riboflavin via FRET. Spectrochim Acta Part A Mol Biomol Spectrosc. 2021;246:119004.
[157] Chen L, Zheng L, Wang F, Yi S, Liu D, Huang X, et al. A ratiometric fluorescence sensor based on metal-organic frameworks and quantum dots for detection of ascorbic acid. Opt Mater (Amst). 2021;121:111622. doi: 10.1016/j.optmat.2021.111622. Epub ahead of print.
[158] Chen J, Jiang S, Wang M, Xie X, Su X. Self-assembled dual-emissive nanoprobe with metal-organic frameworks as scaffolds for enhanced ascorbic acid and ascorbate oxidase sensing. Sens Actuators B Chem. 2021;339:129910. doi: 10.1016/j.snb.2021.129910. Epub ahead of print.
[159] Alilou S, Amirzehni M, Eslami PA. A simple fluorometric method for rapid screening of aflatoxins after their extraction by magnetic MOF-808/graphene oxide composite and their discrimination by HPLC. Talanta. 2021;235:122709. doi: 10.1016/j.talanta.2021.122709. Epub ahead of print.
[160] Zhong X, Zhang M, Guo L, Xie Y, Luo R, Chen W, et al. A dual-signal self-checking photoelectrochemical immunosensor based on the sole composite of MIL-101(Cr) and CdSe quantum dots for the detection of alpha-fetoprotein. Biosens Bioelectron. 2021;189:113389. doi: 10.1016/j.bios.2021.113389. Epub ahead of print.
[161] Xu L, Pan M, Fang G, Wang S. Carbon dots embedded metal-organic framework@molecularly imprinted nanoparticles for highly sensitive and selective detection of quercetin. Sens Actuators B Chem. 2019;286:321–7.
[162] Mahnashi MH, Mahmoud AM, Alhazzani K, AZ A, Algahtani MM, Alaseem AM, et al. Enhanced molecular imprinted electrochemical sensing of histamine based on signal reporting nanohybrid. Microchem J. 2021;168:106439. doi: 10.1016/j.microc.2021.106439. Epub ahead of print.
[163] Qin S-J, Yan B. Dual-emissive ratiometric fluorescent probe based on Eu^{3+}/C-dots@MOF hybrids for the biomarker diaminotoluene sensing. Sens Actuators B Chem. 2018;272:510–7.
[164] Yang JM, Kou YK. Sulfo-modified MIL-101 with immobilized carbon quantum dots as a fluorescence sensing platform for highly sensitive detection of DNP. Inorg Chim Acta. 2021;519:120276. doi: 10.1016/j.ica.2021.120276. Epub ahead of print.
[165] Shi H, Zhang L. A ratiometric fluorescence sensor based on UiO-66-CdTe@ZIF-8 core-shell nanocomposites for the highly selective detection of NO. Res Sq. 2021. doi: 10.21203/rs.3.rs-891851/v1. Epub ahead of print.
[166] Feng JF, Gao SY, Shi J, Liu TF, Cao R. C-QDs@UiO-66-$(COOH)_2$ composite film via electrophoretic deposition for temperature sensing. Inorg Chem. 2018;57:2447–54.
[167] Dong Y, Cai J, Fang Q, You X, Chi Y. Dual-emission of lanthanide metal-organic frameworks encapsulating carbon-based dots for ratiometric detection of water in organic solvents. Anal Chem. 2016;88:1748–52.
[168] Feng H, Liu J, Mu Y, Lu N, Zhang S, Zhang M, et al. Hybrid ultrafiltration membranes based on PES and MOFs @ carbon quantum dots for improving anti-fouling performance. Sep Purif Technol. 2021;266:118586. doi: 10.1016/j.seppur.2021.118586. Epub ahead of print.
[169] Liang R, He Z, Zhou C, Yan G, Wu L. MOF-derived porous Fe_2O_3 nanoparticles coupled with CdS quantum dots for degradation of bisphenol a under visible light irradiation. Nanomaterials. 2020;10:1701. doi: 10.3390/nano10091701. Epub ahead of print.
[170] Pooresmaeil M, Namazi H, Salehi R. Simple method for fabrication of metal-organic framework within a carboxymethylcellulose/graphene quantum dots matrix as a carrier for anticancer drug. Int J Biol Macromol. 2020 Dec 1;164:2301–11.
[171] Xie R, Liu Y, Yang P, Huang L, Zou X, Liu J, et al. 'French fries'-like luminescent metal organic frameworks for the fluorescence determination of cytochrome c released by apoptotic cells and screening of anticancer drug activity. Microchim Acta. 2020;187:221. doi: 10.1007/s00604-020-4207-x. Epub ahead of print.
[172] Chowdhuri AR, Singh T, Ghosh SK, Sahu SK. Carbon dots embedded magnetic nanoparticles @chitosan @metal organic framework as a nanoprobe for pH sensitive targeted anticancer drug delivery. ACS Appl Mater Interfaces. 2016;8:16573–83.
[173] Tabatabaeian K, Simayee M, Fallah-Shojaie A, Mashayekhi F. N-doped carbon nanodots@UiO-66-NH2 as novel nanoparticles for releasing of the bioactive drug, rosmarinic acid and fluorescence imaging. DARU J Pharm Sci. 2019;27:307–15.
[174] Li X, Luo J, Deng L, Ma F, Yang M. *In situ* incorporation of fluorophores in zeolitic imidazolate framework-8 (ZIF-8) for ratio-dependent detecting a biomarker of anthrax spores. Anal Chem. 2020;92:7114–22.
[175] He M, Zhou J, Chen J, Zheng F, Wang D, Shi R, et al. Fe3O4@carbon@zeolitic imidazolate framework-8 nanoparticles as multifunctional pH-responsive drug delivery vehicles for tumor therapy in vivo. J Mater Chem B. 2015;3:9033–42.
[176] Alijani H, Noori A, Faridi N, Bathaie SZ, Mousavi MF. Aptamer-functionalized Fe_3O_4@MOF nanocarrier for targeted drug delivery and fluorescence imaging of the triple-negative MDA-MB-231 breast cancer cells. J Solid State Chem. 2020;292:121680.
[177] Yang D, Yang G, Gai S, He F, Li C, Yang P. Multifunctional theranostics for dual-modal photodynamic synergistic therapy via stepwise water splitting. ACS Appl Mater Interfaces. 2017;9:6829–38.
[178] Liang GX, Zhao KR, He YS, Liu ZJ, Ye SY, Wang L. Carbon dots and gold nanoparticles doped metal-organic frameworks as high-efficiency ECL emitters for monitoring of cell apoptosis. Microchem J. 2021;171:106787. doi: 10.1016/j.microc.2021.106787. Epub ahead of print.
[179] Tabatabaeian K, Simayee M, Fallah-Shojaie A, Mashayekhi F, Hadavi M. Novel MOF-based mixed-matrix membranes, N-CQDs@[Zn(HCOO)3][C2H8N]/PEG, as the effective antimicrobials. J Iran Chem Soc. 2020;17:2987–95.

[180] Zhou Y, Luo Y, Wan J. A CdS quantum dots-sensitized porphyrin-based MOFs for hydrogen evolution reaction in acid media. J Mater Sci Mater Electron. 2020;31:21214–21.
[181] Mao S, Shi J-W, Sun G, Zhang Y, Ji X, Lv Y, et al. Cu (II) decorated thiol-functionalized MOF as an efficient transfer medium of charge carriers promoting photocatalytic hydrogen evolution. Chem Eng J. 2021;404:126533.
[182] Xiao Y-H, Tian W, Jin S, Gu ZG, Zhang J. Host-guest thin films by confining ultrafine Pt/C QDs into metal-organic frameworks for highly efficient hydrogen evolution. Small. 2020;16:2005111.
[183] Mao S, Zou Y, Sun G, Zeng L, Wang Z, Ma D, et al. Thio linkage between CdS quantum dots and UiO-66-type MOFs as an effective transfer bridge of charge carriers boosting visible-light-driven photocatalytic hydrogen production. J Colloid Interface Sci. 2021;581:1–10.
[184] Hao X, Jin Z, Yang H, Lu G, Bi Y. Peculiar synergetic effect of MoS_2 quantum dots and graphene on Metal-Organic Frameworks for photocatalytic hydrogen evolution. Appl Catal B Environ. 2017;210:45–56.
[185] Vaddipalli SR, Sanivarapu SR, Vengatesan S, Lawrence JB, Eashwar M, Sreedhar G. Heterostructured Au NPs/CdS/LaBTC MOFs photoanode for efficient photoelectrochemical water splitting: stability enhancement via CdSe QDs to 2D-CdS nanosheets transformation. ACS Appl Mater Interfaces. 2016;8:23049–59.
[186] Liu N, Tang M, Wu J, Tang L, Huang W, Li Q, et al. Boosting visible-light photocatalytic performance for CO_2 reduction via hydroxylated graphene quantum dots sensitized MIL-101(Fe). Adv Mater Interfaces. 2020;7:2000468.
[187] Wei D, Tang W, Gan Y, Xu X. Graphene quantum dot-sensitized Zn-MOFs for efficient visible-light-driven carbon dioxide reduction. Catal Sci Technol. 2020;10:5666–76.
[188] Li N, Liu X, Zhou J, Chen W, Liu M. Encapsulating CuO quantum dots in MIL-125(Ti) coupled with g-C3N4 for efficient photocatalytic CO_2 reduction. Chem Eng J. 2020;399:125782.
[189] Kong Z-C, Liao J-F, Dong Y-J, Xu YF, Chen HY, Kuang DB, et al. Core@shell $CsPbBr_3$@zeolitic imidazolate framework nanocomposite for efficient photocatalytic CO_2 reduction. ACS Energy Lett. 2018;3:2656–62.
[190] Wu L-Y, Mu Y-F, Guo X-X, Zhang W, Zhang ZM, Zhang M, et al. Encapsulating perovskite quantum dots in iron-based metal-organic frameworks (MOFs) for efficient photocatalytic CO_2 reduction. Angew Chem Int Ed. 2019;58:9491–5.
[191] Qin J, Liu B, Lam K-H, Song S, Li X, Hu X. 0D/2D MXene quantum dot/Ni-MOF ultrathin nanosheets for enhanced N_2 photoreduction. ACS Sustain Chem Eng. 2020;8:17791–9.
[192] Ye H, Li L, Liu D, Fu Q, Zhang F, Dai P, et al. Sustained-release method for the directed synthesis of ZIF-derived ultrafine Co–N–C ORR catalysts with embedded Co quantum dots. ACS Appl Mater Interfaces. 2020;12:57847–58.
[193] Ur Rehman MY, Manzoor S, Nazar N, Abid AG, Qureshi AM, Chughtai AH, et al. Facile synthesis of novel carbon dots@-metal organic framework composite for remarkable and highly sustained oxygen evolution reaction. J Alloys Compd. 2021;856:158038.
[194] Safa S, Khajeh M, Reza Oveisi A, Azimirad R. Graphene quantum dots incorporated UiO-66-NH_2 as a promising photocatalyst for degradation of long-chain oleic acid. Chem Phys Lett. 2021;762:138129.
[195] Si Y, Li X, Yang G, Mie X, Ge L. Fabrication of a novel core-shell CQDs@ZIF-8 composite with enhanced photocatalytic activity. J Mater Sci. 2020;55:13049–61.
[196] Son YR, Kwak M, Lee S, Kim HS. Strategy for encapsulation of CdS quantum dots into zeolitic imidazole frameworks for photocatalytic activity. Nanomaterials. 2020;10:2498. doi: 10.3390/nano10122498. Epub ahead of print.
[197] Sun M, Li F, Zhao F, Wu T, Yan T, Du B, et al. Ionic liquid-assisted fabrication of metal-organic framework-derived indium oxide/bismuth oxyiodide p-n junction photocatalysts for robust photocatalysis against phenolic pollutants. J Colloid Interface Sci. 2022;606:1261–73.
[198] Zargazi M, Entezari MH. Photoelectrochemical water splitting by a novel design of photo-anode: inverse opal-like UiO-66 sensitized by Pd and decorated with S,N graphene QDs. Electrochim Acta. 2021;391:138926. doi: 10.1016/j.electacta.2021.138926. Epub ahead of print.
[199] He Y, Luo S, Hu X, Cheng Y, Huang Y, Chen S, et al. NH2-MIL-125(Ti) encapsulated with *in situ*-formed carbon nanodots with up-conversion effect for improving photocatalytic NO removal and H-2 evolution. Chem Eng J. 2021;420:127643. doi: 10.1016/j.cej.2020.127643. Epub ahead of print.
[200] Liang R, Wang S, Lu Y, Yan G, He Z, Xia Y, et al. Assembling ultrafine SnO_2 nanoparticles on MIL-101(Cr) octahedrons for efficient fuel photocatalytic denitrification. Molecules. 2021;26:7566. doi: 10.3390/molecules26247566. Epub ahead of print.
[201] Li J, Liu L, Liang Q, Zhou M, Yao C, Xu S, et al. Core-shell ZIF-8@MIL-68(In) derived ZnO nanoparticles-embedded In2O3 hollow tubular with oxygen vacancy for photocatalytic degradation of antibiotic pollutant. J Hazard Mater. 2021;414:125395. doi: 10.1016/j.jhazmat.2021.125395. Epub ahead of print.
[202] Kaur R, Vellingiri K, Kim K-H, Paul AK, Deep A. Efficient photocatalytic degradation of rhodamine 6G with a quantum dot-metal organic framework nanocomposite. Chemosphere. 2016;154:620–7.
[203] Kaur R, Rana A, Singh RK, Chhabra VA, Kim KH, Deep A. Efficient photocatalytic and photovoltaic applications with nanocomposites between CdTe QDs and an NTU-9 MOF. RSC Adv. 2017;7:29015–24.
[204] Gan H, Wang Z, Li H, Wang Y, Sun L, Li Y. CdSe QDs@UIO-66 composite with enhanced photocatalytic activity towards RhB degradation under visible-light irradiation. RSC Adv. 2016;6:5192–7.
[205] Wang Q, Wang G, Liang X, Dong X, Zhang X. Supporting carbon quantum dots on NH2-MIL-125 for enhanced photocatalytic degradation of organic pollutants under a broad spectrum irradiation. Appl Surf Sci. 2019;467–468:320–7.
[206] Huang J, Song H, Chen C, Yang Y, Xu N, Ji X, et al. Facile synthesis of N-doped TiO2 nanoparticles caged in MIL-100(Fe) for photocatalytic degradation of organic dyes under visible light irradiation. J Environ Chem Eng. 2017;5:2579–85.
[207] Zhang Y, Li G, Guo QY. CdSe QDs@ Fe-based metal organic framework composites for improved photocatalytic RhB degradation under visible light. Microp Mesop Mater. 2021;324:111291. doi: 10.1016/j.micromeso.2021.111291. Epub ahead of print.
[208] Abd El Khalk AA, Betiha MA, Mansour AS, Abd El Wahed MG, Al-Sabagh AM. High degradation of methylene blue using a

new nanocomposite based on zeolitic imidazolate framework-8. ACS Omega. 2021;6:26210–20.
[209] Li Z, Bu J, Zhang C, Cheng L, Pan D, Chen Z, et al. Electrospun carbon nanofibers embedded with MOF-derived N-doped porous carbon and ZnO quantum dots for asymmetric flexible supercapacitors. New J Chem. 2021;45:10672–82.
[210] Liu S, Zhou J, Cai Z, Fang G, Cai Y, Pan A, et al. Nb_2O_5 quantum dots embedded in MOF derived nitrogen-doped porous carbon for advanced hybrid supercapacitor applications. J Mater Chem A. 2016;4:17838–47.
[211] Yu H, Zhu W, Zhou H, Liu J, Yang Z, Hu X, et al. Porous carbon derived from metal-organic framework@graphene quantum dots as electrode materials for supercapacitors and lithium-ion batteries. RSC Adv. 2019;9:9577–83.
[212] Zhang G, Hou S, Zhang H, Zeng W, Yan F, Li CC, et al. High-performance and ultra-stable lithium-ion batteries based on MOF-derived ZnO@ZnO quantum dots/C core-shell nanorod arrays on a carbon cloth anode. Adv Mater. 2015;27:2400–5.
[213] Li W, Li Z, Yang F, Fang X, Tang B. Synthesis and electrochemical performance of SnOx quantum dots@ UiO-66 hybrid for lithium ion battery applications. ACS Appl Mater Interfaces. 2017;9:35030–9.
[214] Song W, Brugge R, Theodorou IG, Lim AL, Yang Y, Zhao T, et al. Enhancing Distorted metal-organic framework-derived ZnO as anode material for lithium storage by the addition of Ag2S quantum dots. ACS Appl Mater Interfaces. 2017;9:37823–31.
[215] Liu W, Yuan J, Hao Y, Maleki Kheimeh Sari H, Wang J, Kakimov A, et al. Heterogeneous structured MoSe2-MoO3 quantum dots with enhanced sodium/potassium storage. J Mater Chem A. 2020;8:23395–403.
[216] Lu Y, Wang S, Yu K, Yu J, Zhao D, Li C. Encapsulating carbon quantum dot and organic dye in multi-shell nanostructured MOFs for use in white light-emitting diode. Microp Mesop Mater. 2021;319:111062.
[217] Ying W, Mao Y, Wang X, Guo Y, He H, Ye Z, et al. Solid confinement of quantum dots in ZIF-8 for efficient and stable color-conversion white LEDs. ChemSusChem. 2017;10:1346–50.
[218] Gao Y, Hilbers M, Zhang H, Tanase S. Designed synthesis of multiluminescent materials using lanthanide metal-organic frameworks and carbon dots as building-blocks. Eur J Inorg Chem. 2019;2019:3925–32.
[219] Kumagai K, Uematsu T, Torimoto T, Kuwabata S. Photoluminescence enhancement by light harvesting of metal-organic frameworks surrounding semiconductor quantum dots. Chem Mater. 2021;2021(33):1607–17.
[220] Zhu Y-D, Kang Y, Gu Z-G, Zhang J. Step by step bisacrificial templates growth of bimetallic sulfide QDs-attached MOF nanosheets for nonlinear optical limiting. Adv Opt Mater. 2021;9:2002072.
[221] Shi L, Benetti D, Li F, Wei Q, Rosei F. Phase-junction design of MOF-derived TiO_2 photoanodes sensitized with quantum dots for efficient hydrogen generation. Appl Catal B Environ. 2020;263:118317.
[222] Zhang R, Xu J, Jia M, Pan E, Zhou C, Jia M. Ultrafine ZnS quantum dots decorated reduced graphene oxide composites derived from ZIF-8/graphene oxide hybrids as anode for sodium-ion batteries. J Alloys Compd. 2019;781:450–9.
[223] Zhang C, Li W, Li L. Metal halide perovskite nanocrystals in metal-organic framework host: not merely enhanced stability. Angew Chem Int Ed. 2021;60:7488–501.
[224] Hou J, Wang Z, Chen P, Chen V, Cheetham AK, Wang L. Intermarriage of halide perovskites and metal-organic framework crystals. Angew Chem Int Ed. 2020;59:19434–49.